Double Outlet Right Ventricle: Morphology and Function

15

Megha M. Sheth, Yashpal Rana, and Ramiah Rajeshkannan

15.1 Introduction

Conotruncal anomalies represent congenital heart defects resulting from abnormality of formation and/or separation of the outflow tracts of the heart and great vessels. Double outlet right ventricle (DORV) is a type of conotruncal anomaly and includes a wide spectrum of anatomic malformations characterized by the origin of both the aorta and pulmonary arterial trunks entirely or predominately from the morphological right ventricle (RV) [1, 2]. DORV accounts for approximately 1% of all congenital heart disease (CHD).

When an arterial valve or valves override(s) the ventricular septum through a VSD, a "50% rule" is applied [3]. *According to this rule, an overriding arterial trunk is considered as arising from the RV when more than half of the circumference of its valve belongs to the RV.*

As we know that there are three major anatomical segments of heart—i.e., visceroatrial situs, atrioventricular connection, and ventriculoarterial connections. As the term "DORV" describes a form of ventriculoarterial connection, it can occur with any combination of visceroatrial situs and atrioventricular connection, making it an extremely heterogeneous group.

This results in different clinical manifestations and requires a comprehensive diagnostic approach and different surgical management options.

Although echocardiography is considered as an initial imaging modality of choice, it is limited in the reliable assessment because of operator dependency, a small field of view and acoustic window, poor assessment of extracardiac complex vascular anatomy. Catheter angiography is an invasive technique that has several disadvantages including the overlap of adjacent cardiovascular structures and relatively poor depiction of complex intracardiac anatomy. Cross-sectional imaging with Multislice CT (MSCT) or Magnetic Resonance Imaging (MRI) help overcome the limitations of echocardiography and conventional angiography with the ability of simultaneously depicting the systemic and the pulmonary vascular systems. Imaging specialists should be well versed with the complex morphology and physiology of DORV, as well as with various palliative and corrective surgical procedures performed in these patients.

Electronic Supplementary Material The online version of this chapter (https://doi.org/10.1007/978-981-15-6755-1_15) contains supplementary material, which is available to authorized users.

M. M. Sheth (✉) · Y. Rana
U.N. Mehta Institute of Cardiology and Research Centre, Ahmedabad, Gujarat, India

R. Rajeshkannan
Department of Radiology, Amrita School of Medicine, Amrita Institute of Medical Sciences and Research Centre, Amrita Vishwa Vidyapeetham, Kochi, Kerala, India

R. Rajeshkannan et al. (eds.), *CT and MRI in Congenital Heart Diseases*,
https://doi.org/10.1007/978-981-15-6755-1_15

15.2 History

The earliest description of this condition was done in 1793 by Mr. John Abernethy (1764–1831) of London [4]. In 1949, Taussig and Bing reported a case with the aorta arising entirely from the right ventricle and the pulmonary orifice overlaying the ventricular septum through a VSD [5]. Calhoun Witham introduced the specific term "double outlet right ventricle" in 1957 [6].

15.3 Embryology

DORV results from an aberration in the formation of the primary outlet of the heart, i.e., conotruncus, during embryonic development. Chromosomal anomalies such as 22q11.2 deletion syndrome, trisomy 13, trisomy 18, and CHARGE syndrome have been found to be associated with DORV.

15.4 Pathophysiology

The hemodynamic physiology of DORV is extremely complex, VSD being the only source of egress from the left ventricle. The complexity and clinical manifestations revolve around factors like the relationship of the VSD to the arterial valves, size of the VSD, presence or absence of outflow tracts—aortic or pulmonary obstruction and associated anomalies. In the presence of a subaortic VSD, saturated LV blood tends to be directed predominantly to the aorta without significant mixing of RV unsaturated blood. Severe pulmonary stenosis can lead to right to left shunt.

When the VSD is subpulmonary, the aorta is perfused preferentially with deoxygenated systemic venous blood with physiology similar to transposition. The degree of systemic hypoxia is dependent on the adequacy of mixing between blood in the systemic and pulmonary circuits.

The most common mode of presentation is cyanosis usually due to pulmonary outflow obstruction. Tachypnea or difficulty in breathing, poor feeding, slow weight gain, recurrent respiratory tract infections, and failure to thrive are also common. Children without pulmonary obstruction are prone to develop pulmonary arterial hypertension (PAH).

15.5 CT and MR Imaging Techniques

15.5.1 MSCT

Scan Technique Few specific modifications are required from a routine scan. Two runs are recommended to diagnose any abnormal venous drainage—though this depends upon the scanner and institution protocol. ECG-gated scan is preferable to demonstrate complex intracardiac anatomy. Saline chasing bolus to be avoided to get good opacification of the right side of the heart.

All image data should be evaluated using various image reformatting techniques including curved multi-planar reconstruction (c-MPR), maximum intensity projection (MIP), and 3D volume-rendering technique (VRT) to get all the clinically relevant information.

Practical Tips It is important to examine source images as well apart from reconstructed images; as some information might be missed by interpreting only reconstructed images.

Preoperative MSCT with 3D Volume-Rendered (VR) imaging in DORV accurately depicts the following parameters [7]:

- Type of VSD and its relationship to the semilunar valves
- Size of the VSD in relation to the diameter of the pulmonary artery and aorta
- Distance between the VSD and aortic valve
- Distance between the VSD and pulmonary valve

All the above measurements are to be taken and reported, along with routability of the aorta, which is better assessed with MRI.

The morphologic structure and patency of the outflow tracts and presence and severity of sub-

pulmonic obstruction can be well demonstrated on MSCT [8]. Any coexistent anomalies and the state of the extracardiac vascular anatomy can also be evaluated on MSCT. 3D printed heart models with contrast-enhanced CT/MRI in the recent era is revolutionizing surgical outcome [9].

MSCT has proved to be an invaluable diagnostic and decision-making tool as a complement to echocardiography and increasingly as a substitute for invasive angiography in the management of DORV.

15.5.2 MRI Techniques

Cardiac MRI is very useful in preoperative evaluation of complex DORV especially in older children with poor echo windows as well as in postoperative assessment. Recommended MRI protocol include the following sequences:

- Black blood sequences: Spin echo sequences in short-axis, four-chamber, and axial views for evaluation of gross cardiac and extracardiac anatomy, VSD, and pulmonary artery sizes, etc.
- Cine imaging stacks in the four-chamber view, short-axis view, vertical long-axis view, and both ventricular outflow tract view for evaluation of ventricular function, diagnosis of valvular regurgitation and to assess the dynamic relationship between VSD to aorta route. Selected angulated views to image the ventricular septum "en face" has also used.
- Contrast-enhanced Magnetic Resonance angiography (MRA) and respiratory triggered ECG-gated 3D SSFP sequence for evaluation of great vessels and intracardiac anatomy including coronary artery course. The 3D dataset can be used for creating 3D print models.
- Phase-contrast imaging of the main pulmonary artery and the aorta to quantify left-to-right shunts (Q_p:Q_s) and to assess the possible hemodynamic significance of stenosis.

While calculating ventricular volumes, it is important to note that intraventricular baffling or tunneling compromises the RV volume as a part of the RV is incorporated into the LV outflow tract. Therefore, the RV volume needs to be assessed after subtracting the estimated volume of LV to aorta pathway.

Despite the great capabilities of MR imaging for anatomic and functional assessment of the heart, it is time-consuming and may require a lengthy period of patient sedation; hence its use in seriously ill or uncooperative children is often limited. On the other hand, MSCT offers the advantages of short acquisition times and widespread availability.

15.6 Morphology of DORV

To understand the pathophysiology of DORV, it is important to know the morphology of the ventricular outflow tracts.

What is aorto-mitral fibrous continuity?

- The morphologic left ventricle shows fibrous continuity between the aortic and mitral valves. It is well seen on CT scan as a hypodense linear structure between aortic and mitral valves (Fig. 15.1).
- In the morphological right ventricle, there is a muscular structure (ventriculo-infundibular fold) between the pulmonary and tricuspid valves that manifests as discontinuity between the valves (Fig. 15.2).

So if aorto-mitral fibrous continuity is present, then aorta arises from left ventricle and loss of

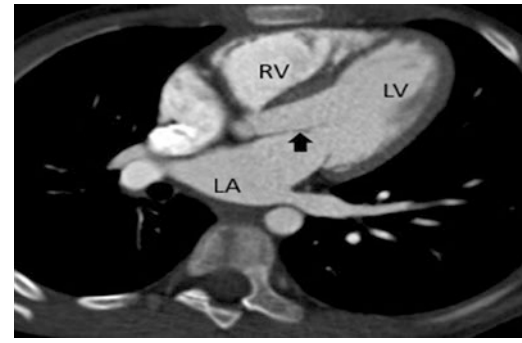

Fig. 15.1 Black arrow shows the aorto-mitral fibrous continuity between aortic and mitral valves

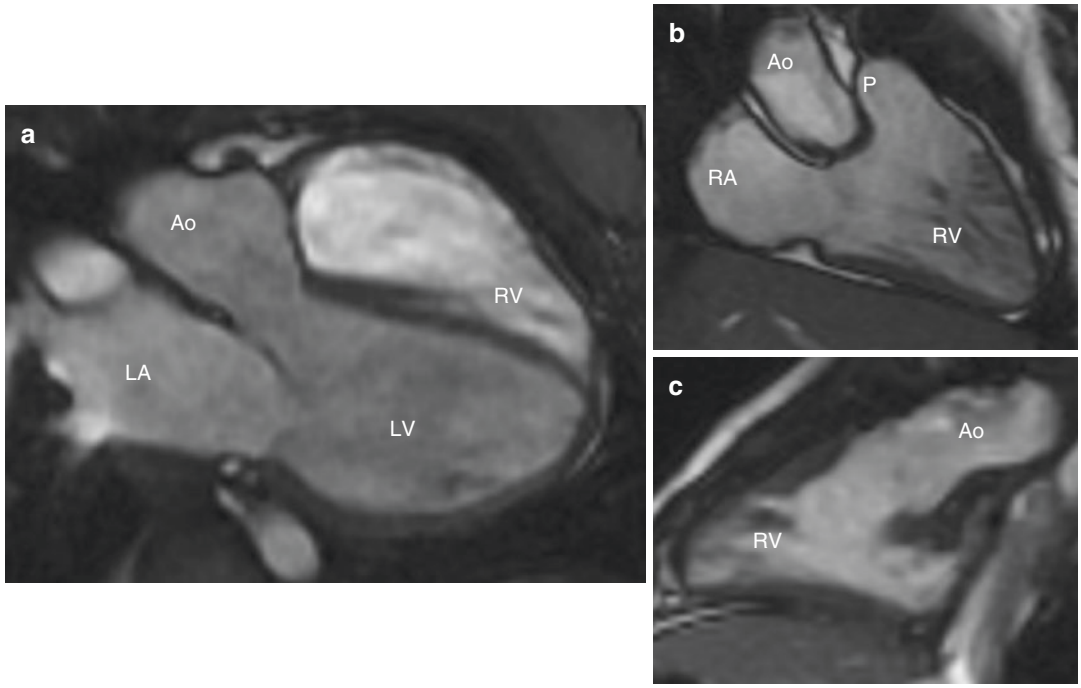

Fig. 15.2 SSFP MRI cine image of LVOT (**a**) shows the normal aorta-mitral fibrous continuity. RVOT view in a normal heart (**b**) and DORV case (**c**) show absent fibrous continuity between the right AV valve and semilunar valve. *Ao* aorta; *LA* left atrium; *LV* left ventricle; *P* pulmonary valve; *RA* right atrium; *RV* right ventricle

aorto-mitral fibrous continuity with subaortic conus is seen in DORV. The conal musculature is usually seen below both great arteries in DORV.

What Is Pulmonary Conus? The pulmonary conus (also known as infundibulum) is a conical muscular pouch formed from the upper and left angle of the right ventricle that supports the leaflets of arterial valve.

The ventriculo-infundibular fold is a muscular structure that is interposed between the leaflets of an atrioventricular and an arterial valve, thereby separates the inlet of the ventricle from its outlet. It is an important landmark for the surgeon as cutting through this muscular fold takes the surgeon outside the heart, and into the transverse pericardial sinus.

The outlet septum, or conal septum, is a muscle that is interposed between the two ventricular outflow tracts. It separates the leaflets of the two arterial valves.

When considering the intracardiac anatomy in DORV, the hearts having both great arteries arising from the right ventricle are not a single spectrum of pathology. More often, there are two infundibular tracts giving rise to both great vessels.

The great arteries can have normal spiraling relationship (subaortic VSD) or be parallel to each other. In most DORV with subpulmonic VSD, the aorta and pulmonary artery are side by side, with D-malposed aorta (aorta on right side). Other less common great arterial relationship includes right and anterior aorta, aorta directly anterior to the pulmonary artery and rarely left and anterior aorta (L malposition) [10].

Almost three-fourths of patients with DORV have some degree of pulmonary stenosis due to narrowing between the outlet septum and the free wall of its infundibulum. Subaortic outflow tract obstruction with or without obstructive lesions of the aortic arch is common in DORV with a sub-

pulmonary VSD. There are multiple distinct groups of cases showing very different intracardiac anatomy.

Different types of VSD are encountered in DORV, based on the relationship of the VSD (subaortic, doubly committed, subpulmonary, or noncommitted) with the great arteries [11]. When the VSD is under the aorta, it is called as subaortic VSD. When the VSD is under the pulmonary artery, it is called as subpulmonic VSD [12]. When the VSD is under both of the great arteries, it is called doubly committed and when the VSD is not near the aorta or the pulmonary artery it is called noncommitted or remote VSD. Schematic diagrams depicting various types of VSD in DORV are shown in Fig. 15.3.

Subaortic VSD is the most common type, followed by subpulmonic VSD, noncommitted VSD, and doubly committed VSD [13–17].

Practical Tips To identify the type of VSD, align the plane along the septum and then view the VSD enface (Fig. 15.4). This is important as the surgeon usually approaches the VSD from the RV side.

15.7 Common Variants of DORV (Summarized in Table 15.1)

15.7.1 Tetralogy of Fallot (TOF)-Like Variant (Figs. 15.5, 15.6, and 15.7)

Tetralogy of Fallot is characterized by anterior, leftward, and superior displacement of the infundibular septum that causes a malaligned VSD, narrowing of the pulmonary outflow tract, overriding of the aortic valve and right ventricular

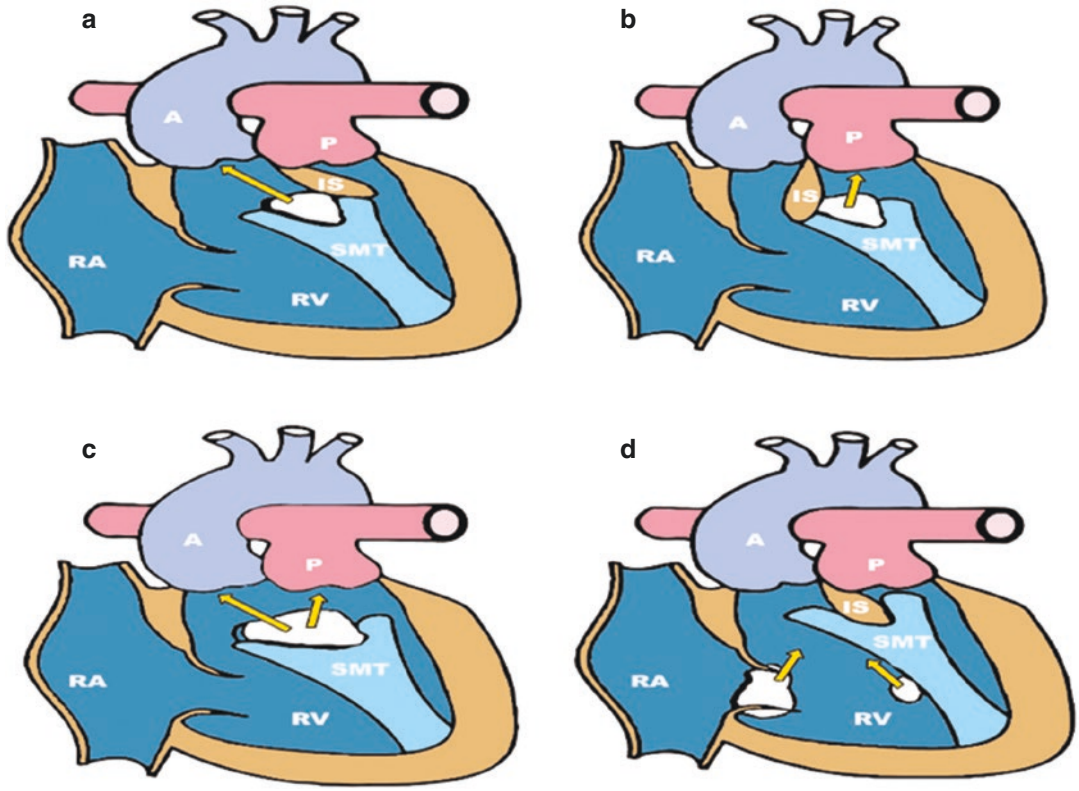

Fig. 15.3 Schematic diagrams depicting various types of VSD. (**a**) Subaortic VSD, (**b**) Subpulmonic VSD, (**c**) Doubly committed VSD, (**d**) Noncommitted VSD. *A* aorta; *P* pulmonary trunk; *RA* right atrium; *RV* right ventricle; *SMT* Septo-Marginal Trabeculae; *IS* infundibular septum

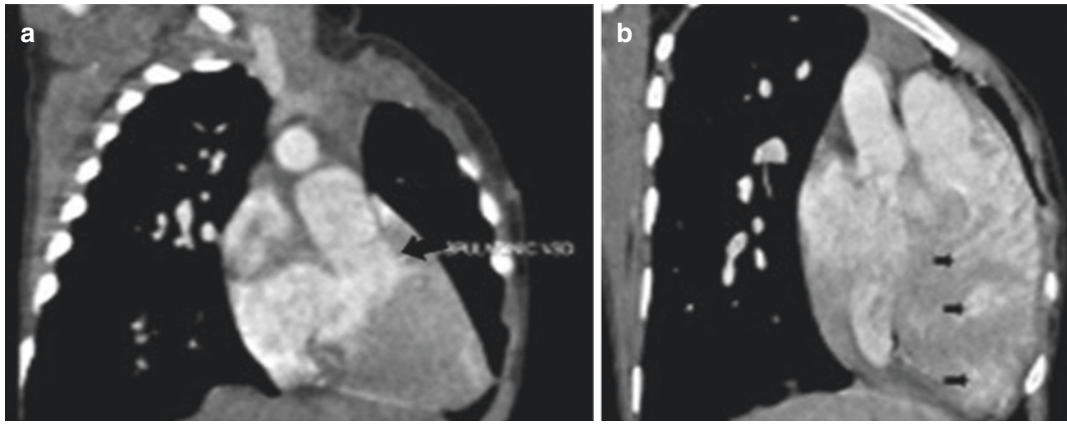

Fig. 15.4 Enface view of the interventricular septum (**a**) showing a subpulmonic VSD (Black arrow) and (**b**) showing multiple mid muscular VSDs (short black arrows)—"*Swiss cheese appearance*"

Table 15.1 Variants of DORV

Common variants
(a) Tetralogy of Fallot (TOF)-like variant consisting of DORV with a subaortic VSD and pulmonary stenosis (PS)
(b) Transposition of great arteries (TGA)-like variant consisting of DORV with a subpulmonic VSD (Taussig–Bing anomaly)
(c) A variant resembling VSD, consisting of DORV with a subaortic VSD but without PS
(d) A variant resembling a univentricular heart
Less frequent variants
(e) with subaortic VSD, aorta left to pulmonary trunk with PS
(f) DORV with noncommitted VSD
(g) DORV with discordant atrioventricular connection
(h) DORV with ambiguous atrioventricular connection
(i) DORV with mirror image atrial arrangement with any of the above combination
(j) DORV without VSD

hypertrophy. Quiet often, more than 50% of the aortic valve overrides the ventricular septum and therefore according to the rule 50% belongs to the right ventricle. TOF and DORV represent two different aspects of the abnormality and are not mutually exclusive.

Hence the variant DORV (TOF type) wherein apart from all the features of TOF, aortic overriding is more than 50% into the right ventricle.

In these subtypes, the VSD is subaortic or doubly committed, with the aorta spiraling from right to left relative to the pulmonary trunk. These children present with clinical features similar to TOF and have progressively worsening cyanosis. Surgical treatment involves the placement of an intraventricular patch to direct left ventricular blood to the aorta and relief of pulmonary obstruction (intracardiac repair).

15.7.2 Transposition of Great Arteries (TGA)-Like Variant (Taussig–Bing Anomaly) (Figs. 15.8, 15.9, 15.10, 15.11, and 15.12)

Transposition of the great arteries (TGA) is another form of ventriculoarterial connection in which the pulmonary arterial trunk arises from the morphological left ventricle and the aorta arises from the morphological right ventricle, i.e., ventriculoarterial discordance.

DORV (TGA type) occurs when the aorta is arising from the right ventricle with subaortic conus and the pulmonary artery arises predominantly from the right ventricle with a subpulmonic VSD. Hypertrophy of the infundibular septum and parietal band may lead to subaortic obstruction and may also be associated with coarctation of the aorta.

The children are cyanosed in the newborn period and are prone to develop early pulmo-

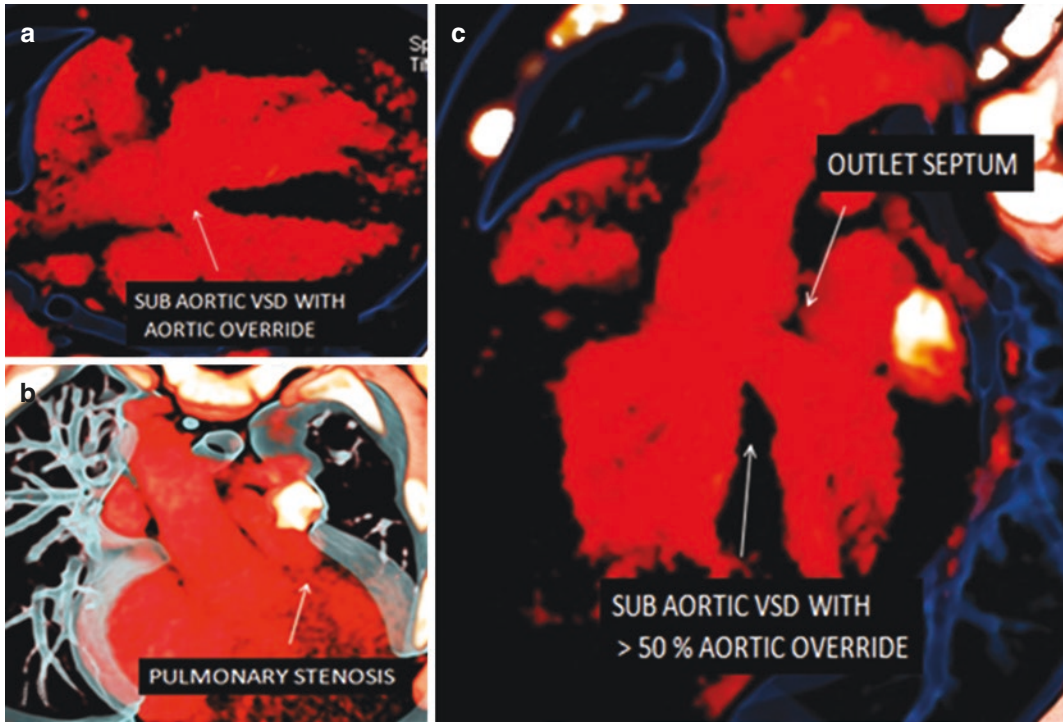

Fig. 15.5 TOF-like variant—DORV with subaortic VSD and PS. VRT thin images showing (**a**) subaortic VSD, (**b**) pulmonary stenosis, (**c**) >50% aortic override

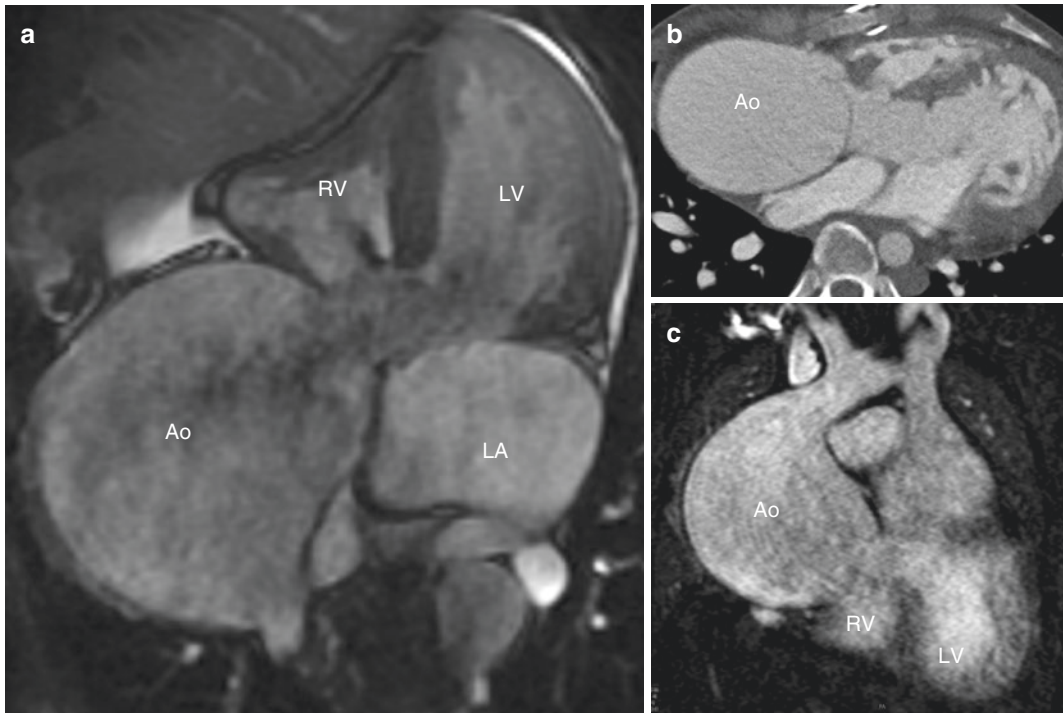

Fig. 15.6 A 28-year-old male with DORV. Oblique axial SSFP (**a**), oblique axial CT (**b**) and coronal MRA (**c**) show DORV, subaortic VSD, aneurysmally dilated ascending aorta, aortic stenosis, and severe aortic regurgitation. *Ao* aorta; *LA* left atrium; *LV* left ventricle; *RV* right ventricle (Ref to Videos 15.1, 15.2, 15.3, 15.4, and 15.5)

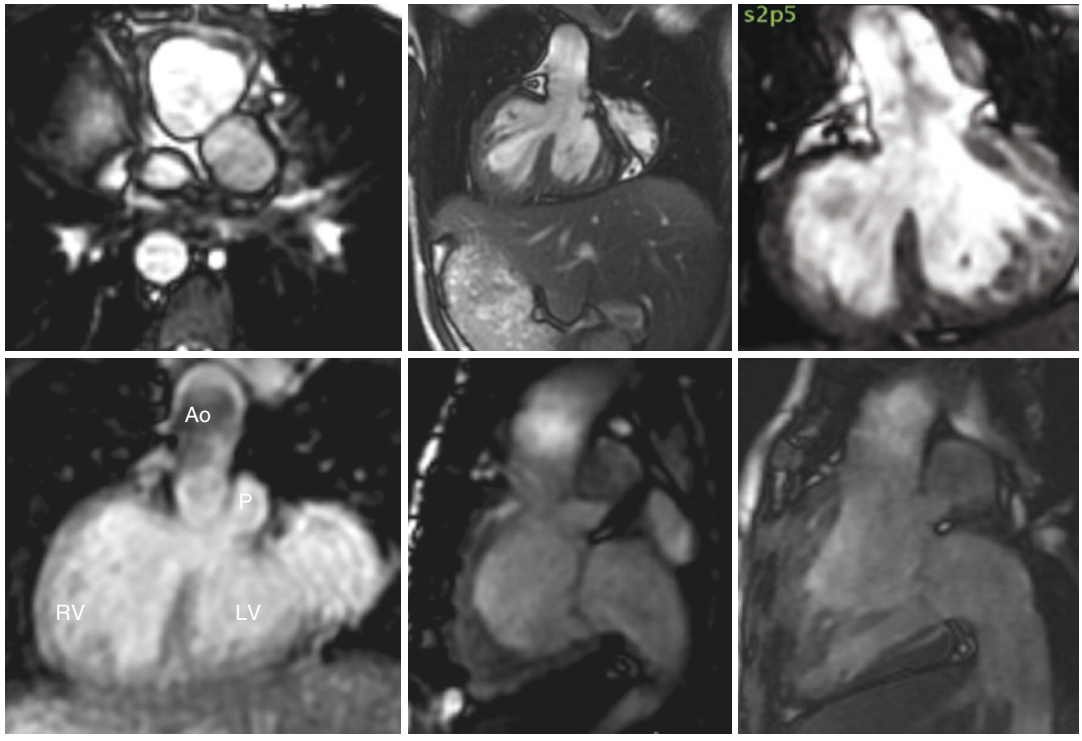

Fig. 15.7 A 17-year-old girl with DORV, situs inversus, dextrocardia, and d-malposed great arteries. VSD is doubly committed, but predominantly committed to the aorta with pulmonary stenosis (Ref to Videos 15.6, 15.7, 15.8, 15.9, 15.10, 15.11, and 15.12)

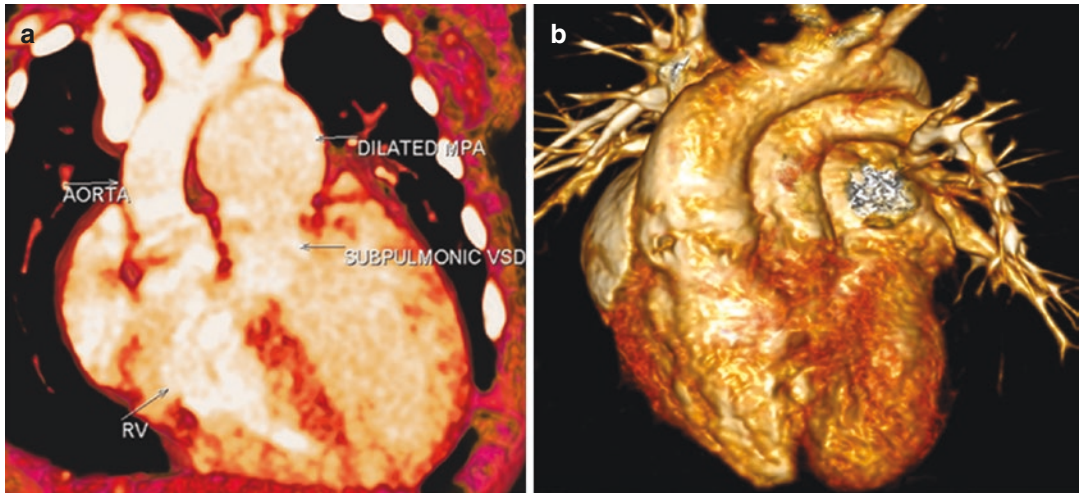

Fig. 15.8 TGA-like variant—DORV with a subpulmonic VSD (Taussig–Bing anomaly). (**a**) VRT thin image, (**b**) 3D VRT image showing DORV with a subpulmonic VSD

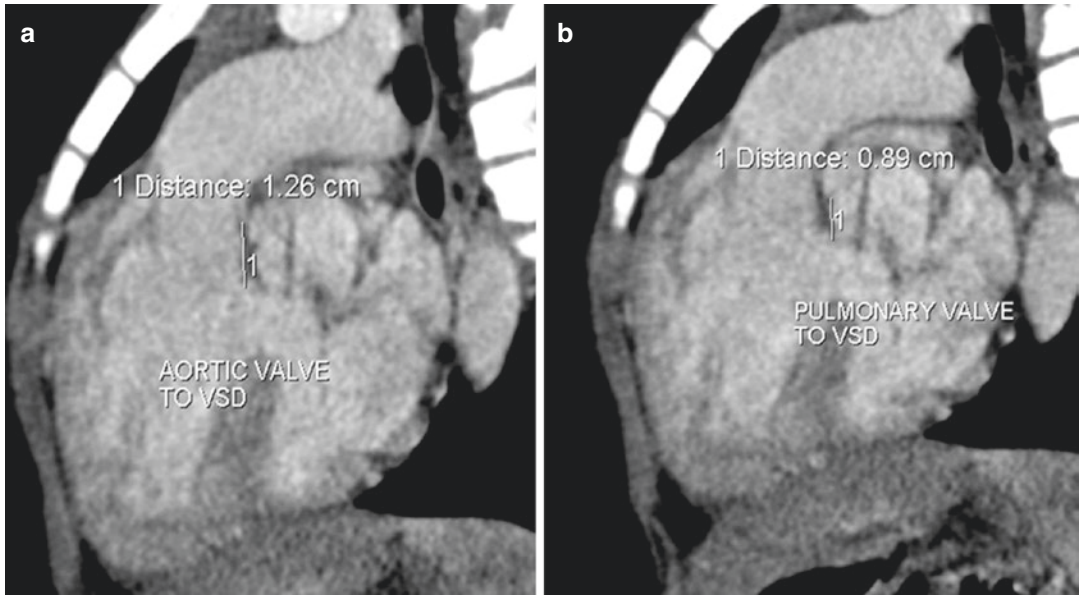

Fig. 15.9 DORV with subpulmonic VSD and PS. Coronal oblique images showing (**a**) aortic annulus to the upper border of VSD distance, (**b**) pulmonary annulus to upper border of VSD distance

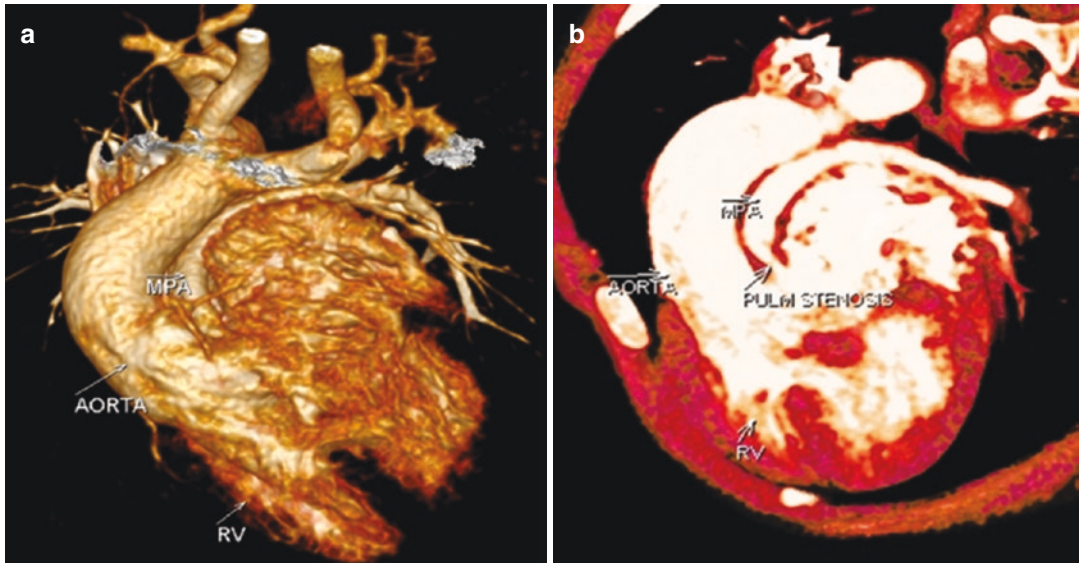

Fig. 15.10 DORV with subpulmonic and noncommitted mid-muscular VSDs. (**a**) 3D VRT, (**b**) VRT thin image

nary hypertension. It is treated by placing a patch to connect the LV to the pulmonary artery and an "Arterial Switch" operation (as for TGA) may be done so that the left ventricle is connected to the aorta and the RV to the pulmonary circulation.

15.7.3 Variant Resembling VSD (Fig. 15.13)

In this variant of DORV, the VSD is usually subaortic or doubly committed and no pulmonary stenosis. These children may not have cya-

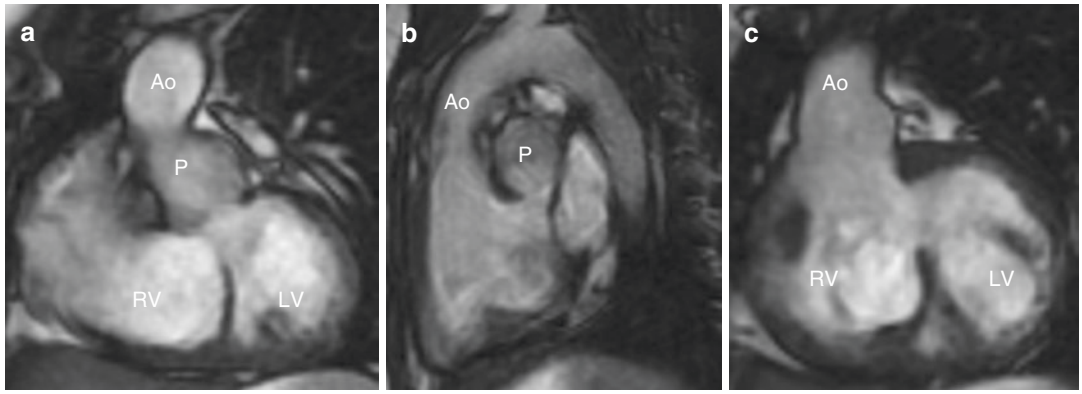

Fig. 15.11 A 11-year-old girl with TGA type of DORV. Pulmonary trunk (P) overriding the large conoventricular VSD (**a**), aorta (Ao) is directly anterior to the pulmonary artery (**b**). LV to aorta appears routable through the VSD (**c**)

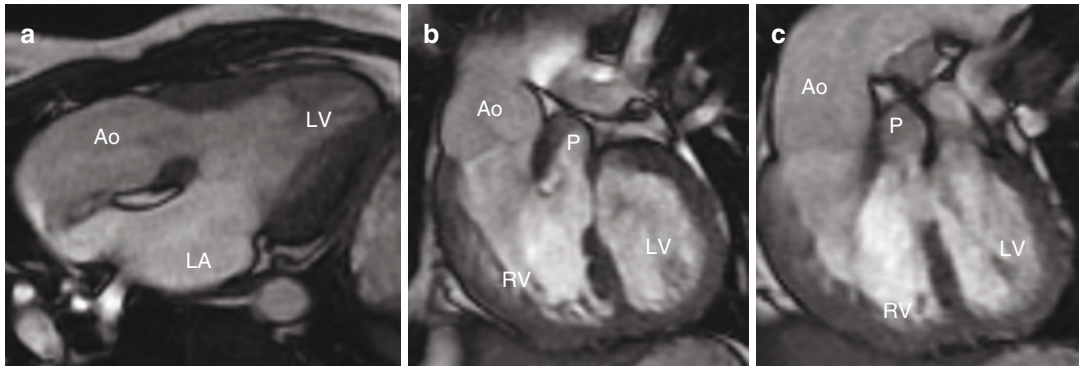

Fig. 15.12 A 17-year-old female with DORV, subpulmonary VSD, and pulmonary stenosis. Three chamber SSFP (**a**) and outflow SSFP MRI (**b**, **c**) show a large conoventricular VSD with some superior inlet extension. Long LV to aorta route with tricuspid and subaortic conal tissue along the pathway. Tricuspid valve also attached to subaortic conal septum. *Ao* aorta; *LA* left atrium; *LV* left ventricle; *P* pulmonary artery; *RV* right ventricle (Ref to Videos 15.13, 15.14, 15.15, 15.16, 15.17, 15.18, and 15.19)

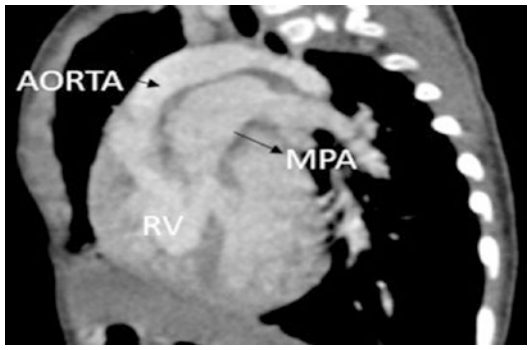

Fig. 15.13 Variant resembling VSD-DORV with subpulmonic VSD but without pulmonary stenosis

nosis, but develop early pulmonary arterial hypertension as there is increased flow to the pulmonary circulation. Repair involves the placement of an intraventricular patch to direct left ventricular blood to the aorta.

15.7.4 Variant Resembling a Univentricular Heart (Figs. 15.14, 15.15, and 15.16)

In this variant of DORV, there is a single dominant ventricle of RV morphology with aplastic/hypoplastic LV and both great vessels arising from the dominant ventricle of RV morphology.

This is also found to be associated with AV cushion defects and double inlet of dominant RV.

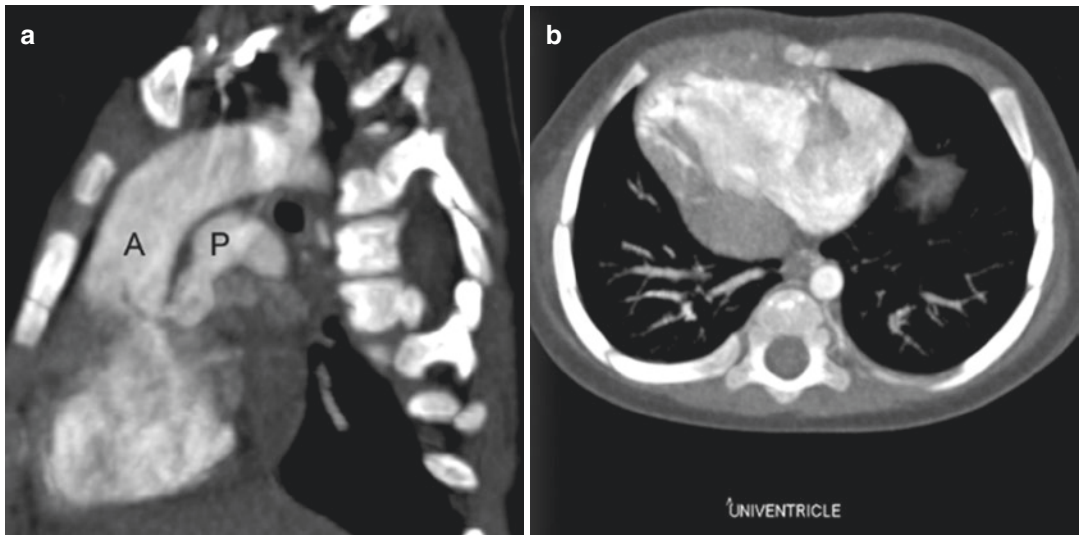

Fig. 15.14 DORV variant with univentricular morphology. (**a**) Sagittal oblique MIP image, (**b**) Axial oblique MPR image. *A* aorta; *P* pulmonary trunk

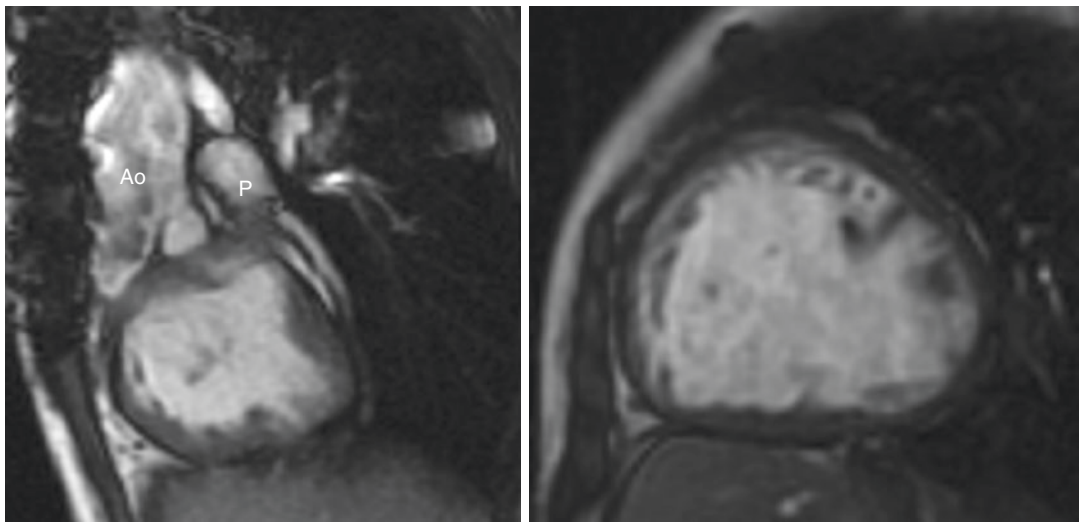

Fig. 15.15 A 10-year-old girl with single ventricle and DORV. *Ao* aorta; *P* pulmonary artery

15.8 Less Frequent Variants of DORV

15.8.1 DORV with Subaortic VSD, Aorta Left to Pulmonary Trunk with PS (Figs. 15.17 and 15.18)

The key point in diagnosing this variant is that, despite the aorta being left-sided, the heart exhibits its usual atrial arrangement with concordant AV connections. So, this entity is an exception to loop rule. In these cases, VSD is usually subaortic, so it is considered amenable for corrective surgery. Great arteries are parallelly arranged [18].

15.8.2 DORV with Noncommitted VSD (Fig. 15.19)

When the distance between VSD and the two arterial valves was greater than the diameter of the aortic valve, it is termed a noncommitted VSD [19].

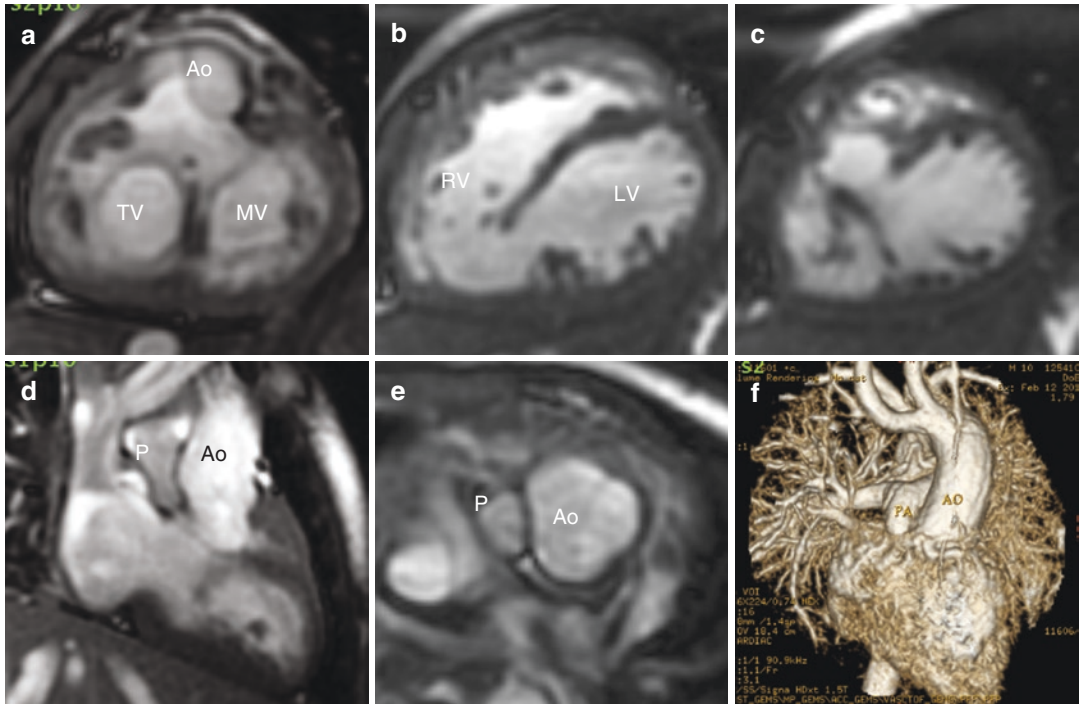

Fig. 15.16 A 10-year-old boy with DORV and multiple VSD at conoventricular (**a**), posterior (**b**), and apical muscular (**c**) regions. L-malposed aorta with severe pulmonary stenosis (**d**–**f**). The complex intracardiac anatomy with multiple large VSDs and severe pulmonary stenosis make him unsuitable for biventricular repair. So he was recommended to undergo single ventricle Fontan pathway of palliation. *Ao* aorta; *LV* left ventricle; *MV* mitral valve; *P* pulmonary artery; *RV* right ventricle; *TV* tricuspid valve

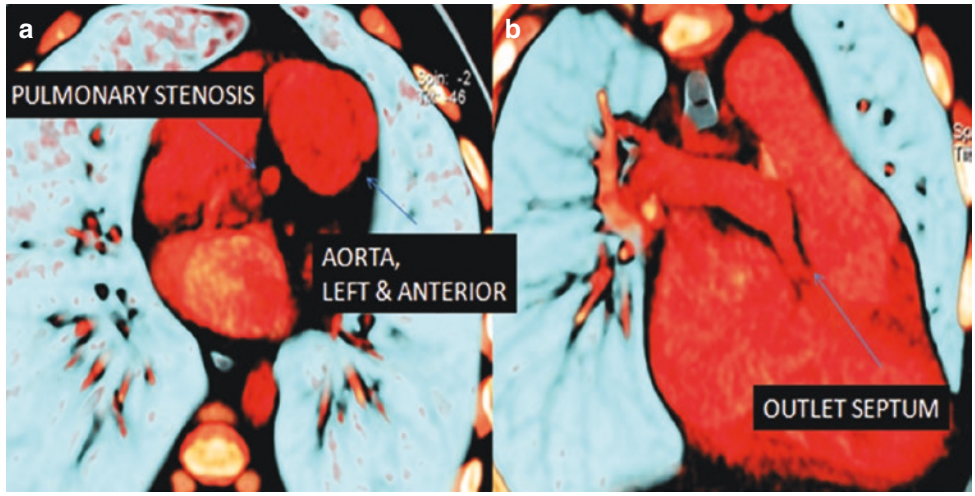

Fig. 15.17 DORV with subaortic VSD, aorta left to pulmonary trunk with PS. (**a**) VRT thin image showing aorta left to the pulmonary trunk, (**b**) VRT thin image showing PS and outlet septum

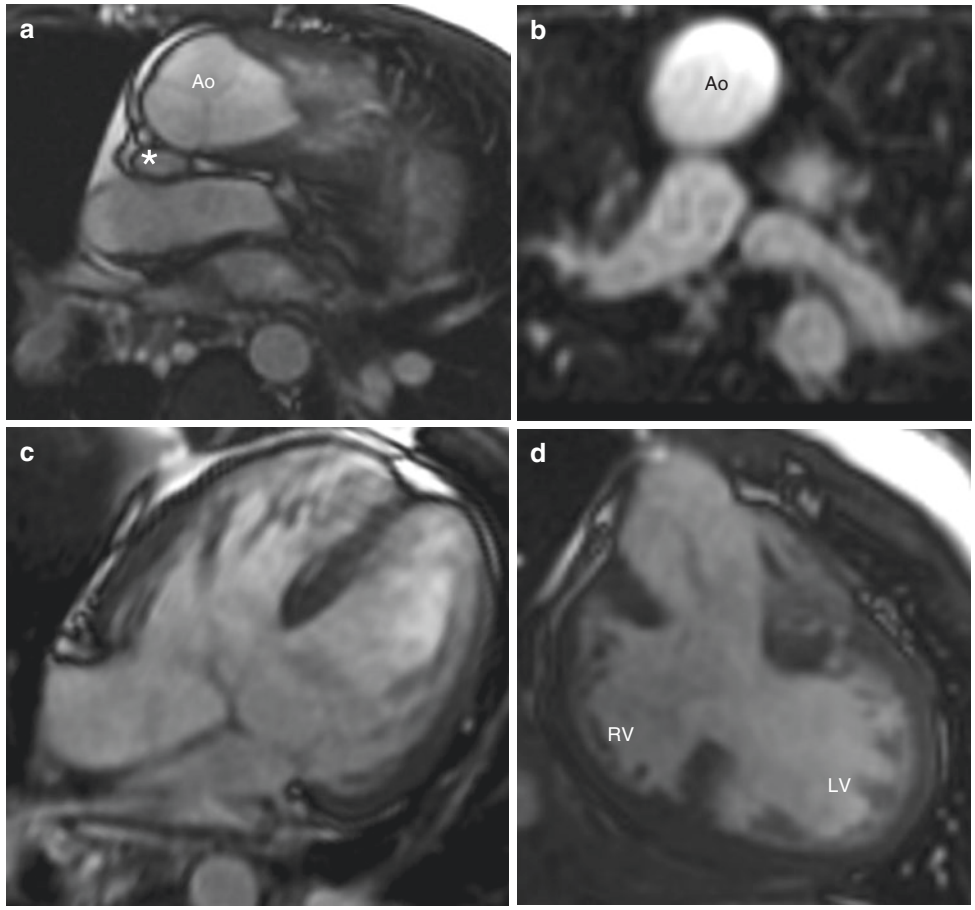

Fig. 15.18 A 12-year-old boy with DORV L-malposed aorta (Ao), severe pulmonary stenosis (*), nonconfluent pulmonary arteries (**b**), large inlet VSD (**c**) with conoventricular extension. LV appears routable to aorta across the VSD with a long patch (**d**)

The remoteness of the VSD from the arterial valves is determined by the location of the VSD within the septum and also by the extent of the muscular infundibulum.

As already explained earlier, the VSD is the only egress of the left ventricle in DORV. Hence, its small size implies left ventricular outflow tract obstruction [20, 21]. The VSD is considered restrictive when the diameter of the defect is smaller than the diameter of the aortic valve [22]. A restrictive VSD is seen in approximately 10% of DORV cases, most commonly occurring in the variety with a noncommitted VSD [23].

15.8.3 DORV with Discordant Atrioventricular Connection (Figs. 15.20 and 15.21)

This variant mimics congenitally corrected TGA (CCTGA) as the right atrium connects to the anatomic left ventricle, left atrium connects to the anatomic right ventricle, but both great arteries arise completely from the anatomic right ventricle [24]. These two entities were thought to differ only in the grade of overriding of the posterior pulmonary artery. There is a higher incidence of dextrocardia and L-malposed great arteries.

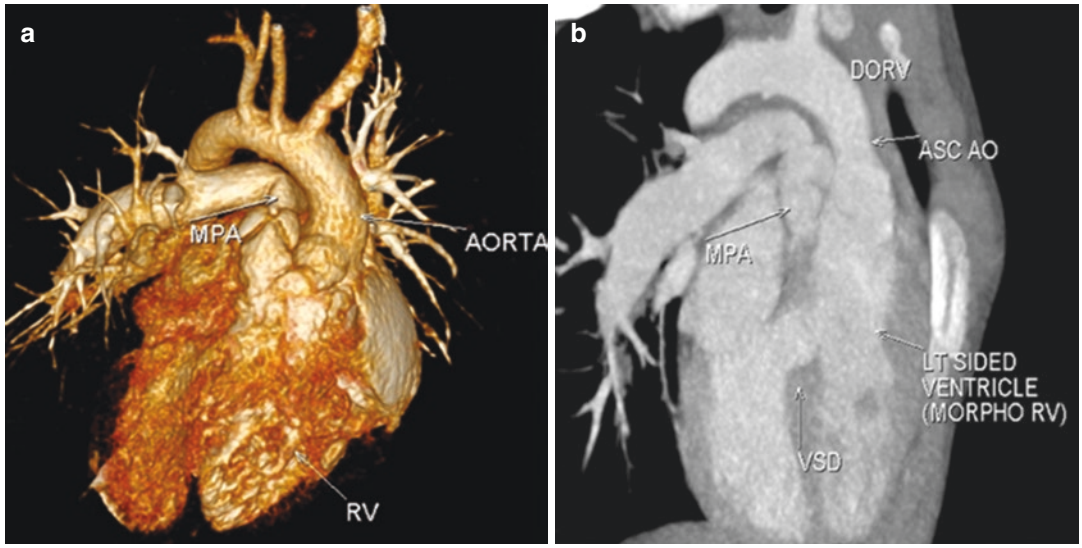

Fig. 15.19 DORV with discordant atrioventricular connection (Aorta left to the pulmonary trunk) and noncommitted VSD. (**a**) 3D VRT image, (**b**) coronal oblique MIP image

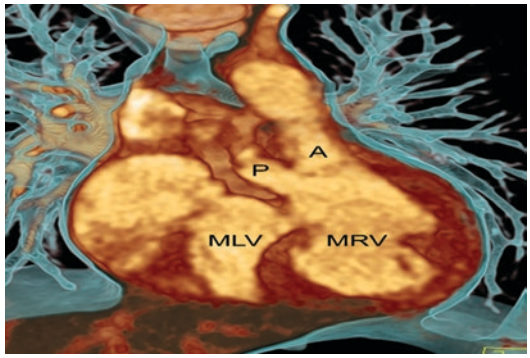

Fig. 15.20 Coronal oblique VRT thin image showing DORV with discordant atrioventricular connection (L-loop ventricle) and L-malposed aorta (aorta left to pulmonary trunk). *A* aorta; *P* pulmonary trunk; *MRV* morphological right ventricle; *MLV* morphological left ventricle

DORV with AV discordance is more prone to present with VSD and subvalvular pulmonary stenosis, while those with CCTGA have a greater likelihood of presenting with tricuspid regurgitation and atrioventricular block.

15.8.4 DORV with Mirror-Image Atrial Arrangement (Fig. 15.22)

In situs inversus, the internal organs including atria show mirror image arrangement. Along with mirror-imaged atrial arrangement, any of the previously mentioned DORV variations may occur.

15.8.5 DORV with Isomeric Atrial Appendages (Ambiguous AV Connection)

Double outlet right ventricle is frequent in the presence of isomeric atrial appendages, being particularly common in the overall group of patients having isomeric right appendages. When DORV occurs in the setting of heterotaxy, other associated abnormalities including pulmonary venous anomalies are to be assessed (Figs. 15.23 and 15.24).

15.8.6 DORV Without VSD

Very rarely DORV occurs with an intact ventricular septum [20]. This variety is usually associated with severe hypoplasia/atresia of the mitral valve and left ventricle. Most of the reported cases show findings suggesting spontaneous closure of the restrictive VSD postnatally or during fetal life [20].

Practical Tips Why is it important to differentiate all the subtypes of DORV?—Because each type of DORV is managed in different ways.

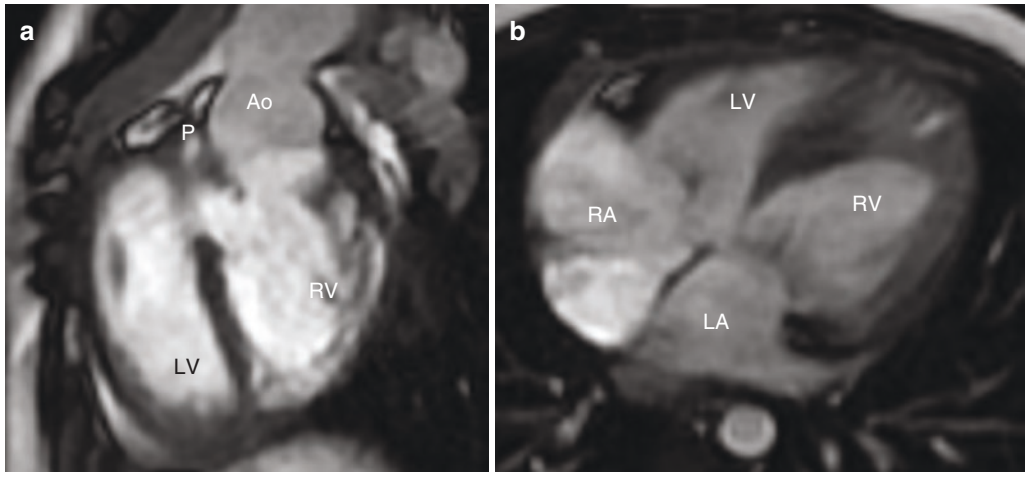

Fig. 15.21 An 8-year-old child with DORV and AV discordance (L loop ventricle). Outflow view (**a**) and four-chamber MRI (**b**) show both great arteries are arising from the left-sided morphological RV. *Ao* aorta; *LA* left atrium; *LV* left ventricle; *P* pulmonary artery; *RA* right atrium; *RV* right ventricle (Ref to Videos 15.20, 15.21, 15.22, 15.23, and 15.24)

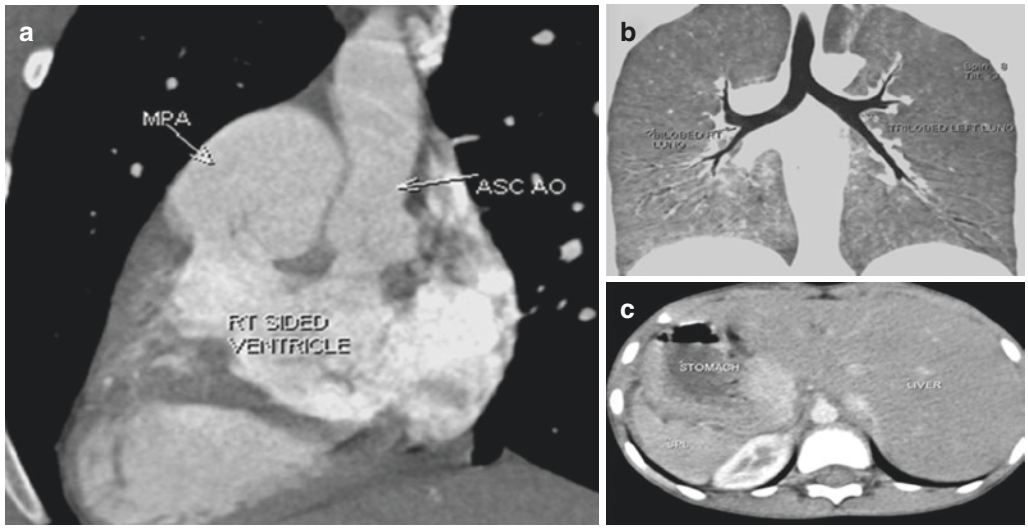

Fig. 15.22 DORV with situs inversus. (**a**) Coronal oblique MIP image showing DORV, (**b**) Coronal MinIP image showing inverted bronchial branching pattern, (**c**) axial MPR image showing spleen and stomach on the right side while liver on left side

15.9 Associated Other Cardiac Anomalies

Commonly observed associated cardiac anomalies are endocardial cushion defects or atrioventricular canal defects (AVCD) (Fig. 15.25), coarctation of the aorta (Fig. 15.26), transposition of great arteries, abnormal pulmonary venous drainage (Fig. 15.27), juxtaposition of atrial appendages (Fig. 15.28), aortopulmonary window (Fig. 15.29), coronary anomaly (Fig. 15.30), right side aortic arch, double aortic arch (Fig. 15.31), and mitral valve problems. Extracardiac anomalies, such as heterotaxy (polysplenia, asplenia, situs ambiguous) and intestinal malrotation, are frequent.

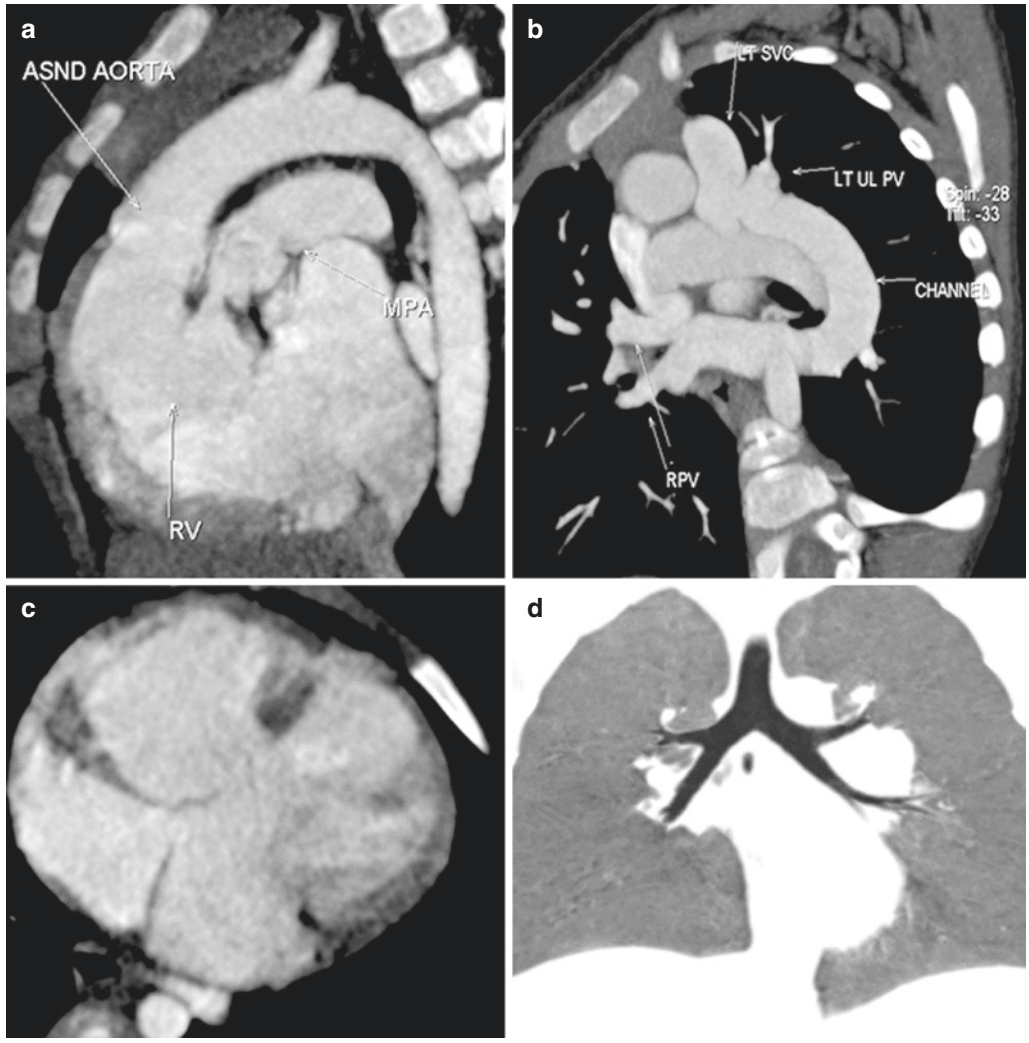

Fig. 15.23 DORV with complete AVCD, TAPVC, and right isomerism (**a**) Coronal oblique MIP image showing DORV, (**b**) coronal oblique MIP image showing supracardiac TAPVC, (**c**) axial MPR image showing complete AVCD—atrioventricular canal defect, (**d**) coronal MinIP image showing bilateral eparterial bronchi

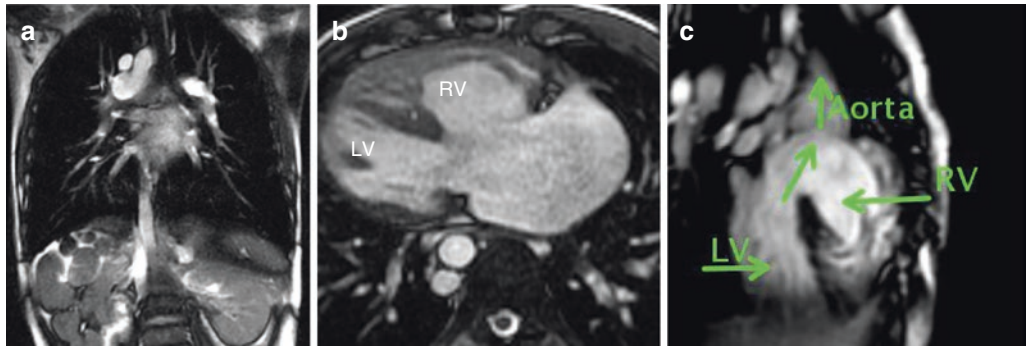

Fig. 15.24 A 12-year-old child with left isomerism (polysplenia, both side hyparterial bronchi) (**a**), dextrocardia, complete AV canal defect (**b**). Both great arteries are arising from the left-sided morphological RV with clear LV to aorta route (**c**) (Ref to Videos 15.25, 15.26, 15.27, 15.28, 15.29, 15.30, 15.31, and 15.32)

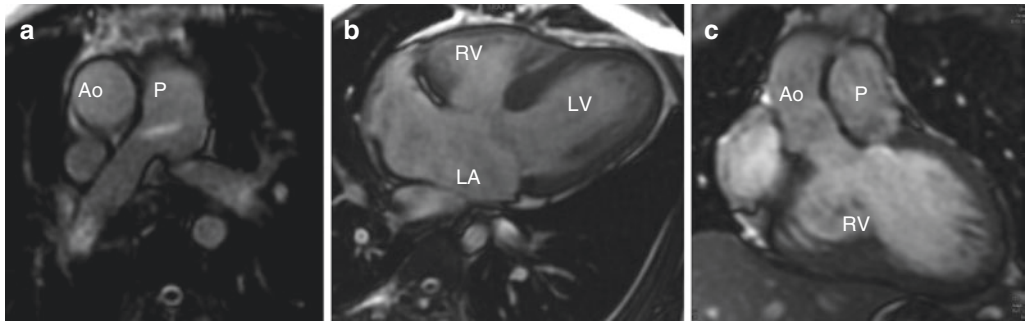

Fig. 15.25 A 39-year-old patient with DORV, D-malposed aorta (**a**), common atrium, Common AV valve, hypoplastic RV (**b**), both great arteries come from RV with severe infundibular pulmonary stenosis (**c**). *Ao* aorta; *LA* left atrium; *LV* left ventricle; *P* pulmonary artery; *RV* right ventricle

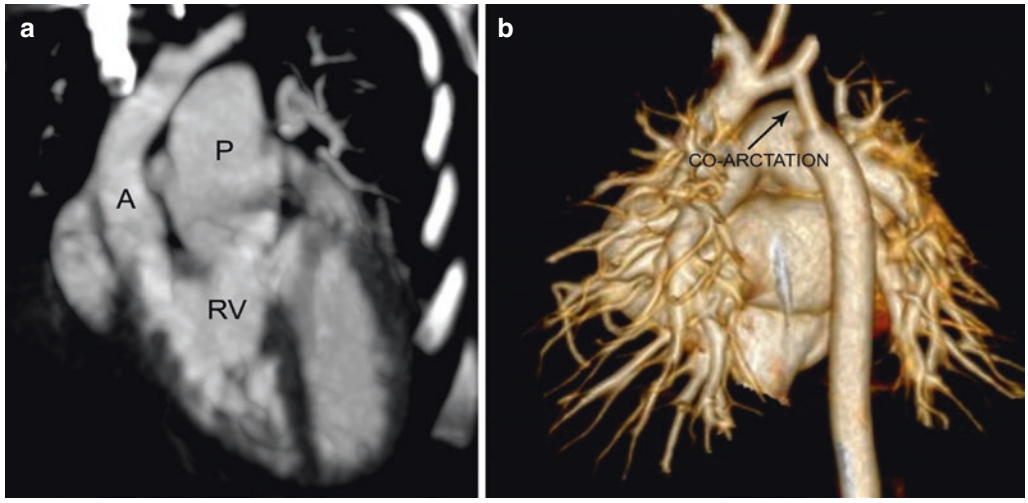

Fig. 15.26 DORV with juxta-ductal coarctation of aorta (**a**) coronal oblique MIP image, (**b**) 3D VRT image. *A* aorta; *P* pulmonary trunk; *RV* right ventricle

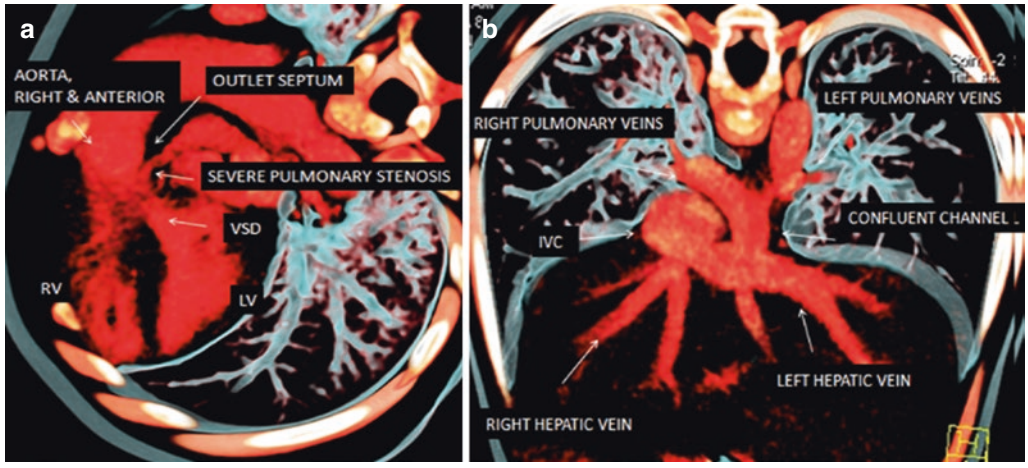

Fig. 15.27 DORV with infracardiac TAPVC (**a**) VRT thin image showing DORVwith PS, (**b**) VRT thin image showing Infracardiac TAPVC

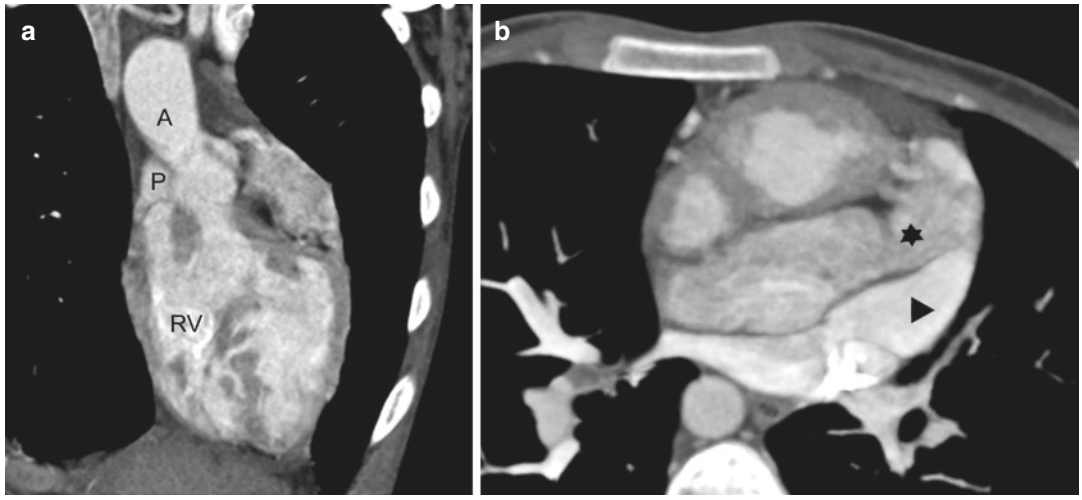

Fig. 15.28 DORV with L-juxtaposed both atrial appendages (**a**) coronal oblique MIP image showing DORV, (**b**) axial MPR image showing L-juxtaposed both atrial appendages. *A* aorta; *P* pulmonary trunk. Star mark denotes right atrial appendage. Arrowhead mark denotes left atrial appendage

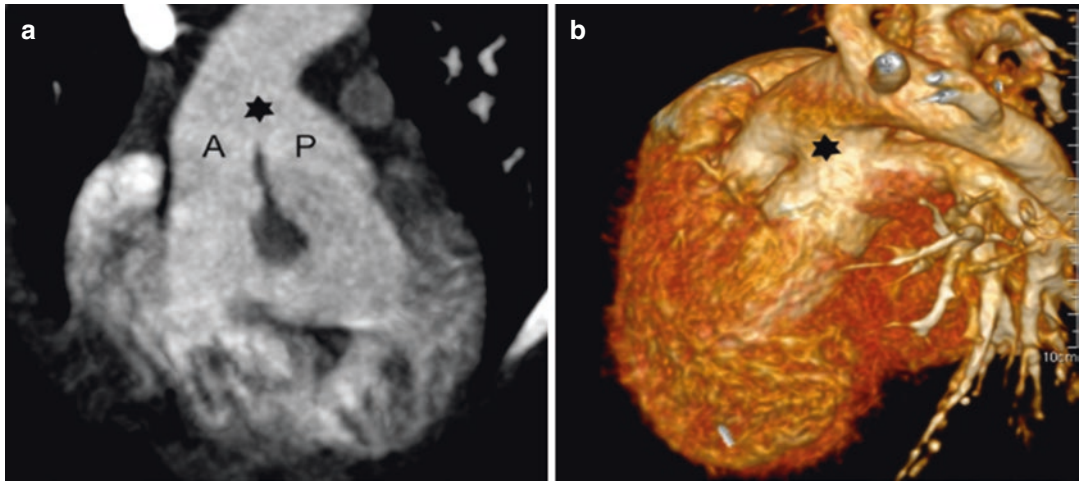

Fig. 15.29 DORV with type-I proximal AP (aortopulmonary) window. (**a**) Coronal oblique MIP image, (**b**) 3D VRT image. *A* aorta; *P* pulmonary trunk. Star mark denotes AP window

15.9.1 Juxtaposition of the Atrial Appendages (Fig. 15.28)

Juxtaposition is a condition where the whole or part of the appendage of one atrium is displaced to the other. The left juxtaposition of the right atrial appendage is much more common than the right juxtaposition [25].

Awareness of this rare condition is important as the unusual atrial anatomy may complicate the surgical procedure when the atrial septal defect needs to be closed or when intra-atrial rerouting of the pulmonary or systemic venous pathways is required.

15.9.2 Abnormalities of the Atrioventricular Valves

Straddling or overriding of the tricuspid valve, mitral valve, or both valves is not frequent.

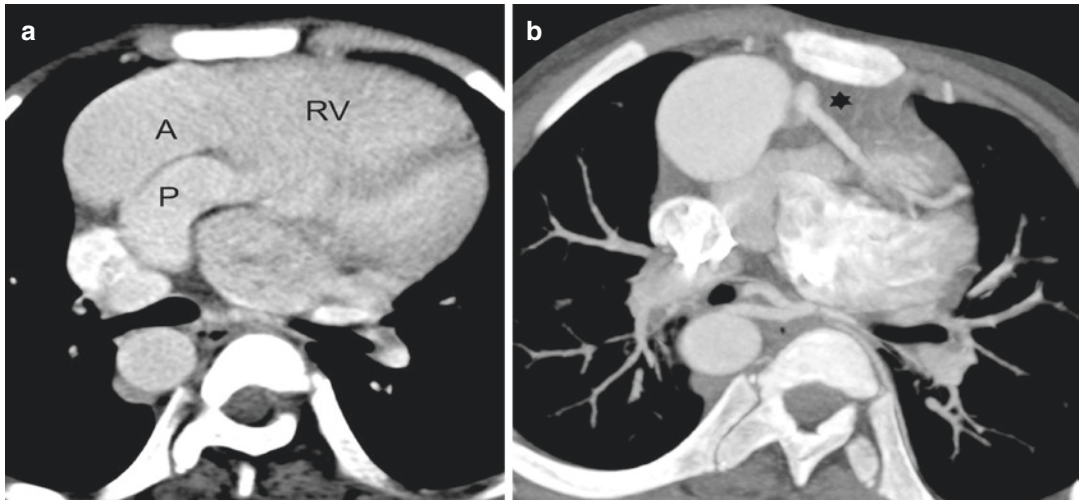

Fig. 15.30 DORV with coronary anomaly (**a**) Axial oblique MIP image showing DORV, (**b**) axial oblique MIP image showing coronary crossing RVOT. *A* aorta; *P* pulmonary trunk; *RV* right ventricle. Star mark denotes coronary crossing RVOT

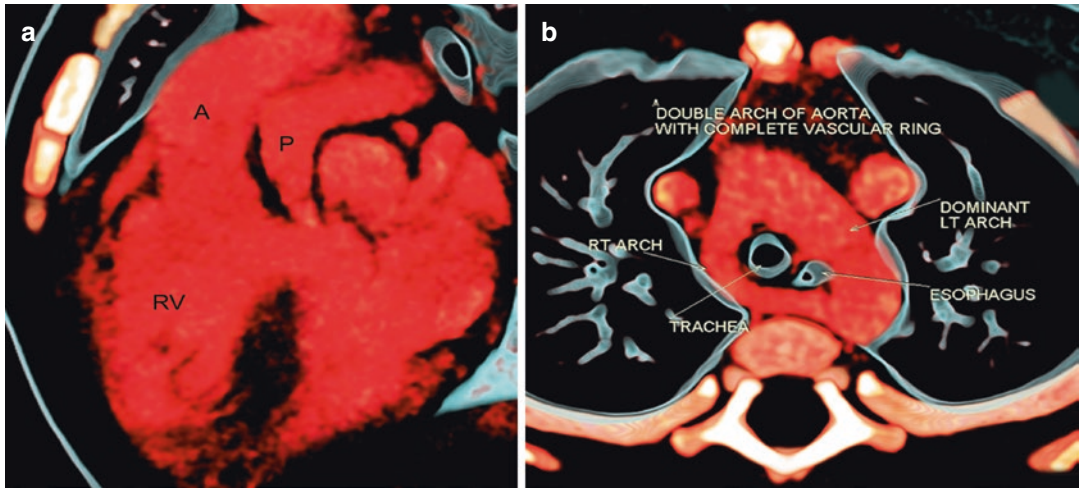

Fig. 15.31 DORV with a double aortic arch. (**a**) VRT thin image showing DORV with PS, (**b**) VRT thin image showing double aortic arch encircling trachea and esophagus

15.10 3D Printing in DORV

DORV with two ventricles and remote VSD still represents a significant therapeutic challenge [26]. The critical aspect of baffling the left ventricular outflow through the VSD to the aorta is sometimes challenging to assess completely on the basis of information obtained from conventional echocardiography. Recently, virtual 3D heart models generated from cardiac MR or CT datasets have been used to delineate the intracardiac anatomy in complex DORV [27, 28].

15.11 Surgical Repair [29–33]

The ideal surgery is biventricular repair by connecting the morphological left ventricle (LV) to the aorta through the VSD and the morphological RV to the pulmonary artery, that leaves the patient with functioning right and left ventricles. The orientation of the VSD is critical for selecting the appropriate surgical approach to avoid obstructing a newly created subaortic or subpulmonary outflow channel. In addition to VSD and its relation to great arteries, outflow tract obstruction, chordal attachments of atrioventricular valves, and the distance between the tricuspid and pulmonary valve will also determine the surgical approach (Figs. 15.32, 15.33, and 15.34).

Indications for single ventricle pathway surgery (Fontan correction) includes hypoplasia of one of the ventricle (Fig. 15.35), substantial straddling of an atrioventricular valve, significant atresia of the mitral valve, large AV canal defect, and extremely unroutable VSD [34].

Various common surgical strategies depending on the DORV variant are as shown in Table 15.2.

15.11.1 LV to Aorta Routability

The goal of surgical correction is to connect ventricle to the great artery, without compromising AV valve function, without outflow obstruction, without compromising ventricular volume and function and avoiding injury to the conduction pathway. Advanced echo, MRI, and 3D models are very useful to achieve the goal. The following parameters are checked to assess the routability:

- Type of VSD
- Conal septum—prominent/hypoplastic, deviation and outflow obstruction
- AV valve anatomy—complete AV canal defect, straddling/overriding, attachment of leaflet to conal septum
- VSD to semilunar valve distance
- Tricuspid to pulmonary valve distance

15.11.2 Postoperative Complications

Complications after DORV repair include residual VSD, ventricular outflow tract obstruction, semilunar valve stenosis/regurgitation, homograft

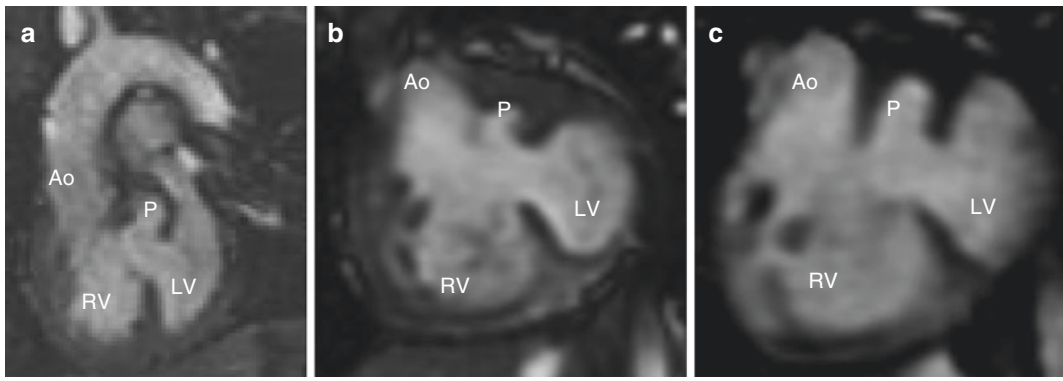

Fig. 15.32 A 6-year-old boy with DORV. Outflow view (**a**) and basal short axis view (**b**, **c**) show DORV, severe PS, Large CV VSD with inlet extension, two good size ventricles, and function. VSD is routable to the aorta with about 1 cm subaortic conus to be excised. Surgery was performed with the routing of VSD to aorta, infundibular and conal septum resection and Rastelli procedure. He developed complete heart block 25 days after surgery and managed with a permanent pacemaker. *Ao* aorta; *LV* left ventricle; *P* pulmonary artery; *RV* right ventricle (Ref to Videos 15.33, 15.34, 15.35, and 15.36)

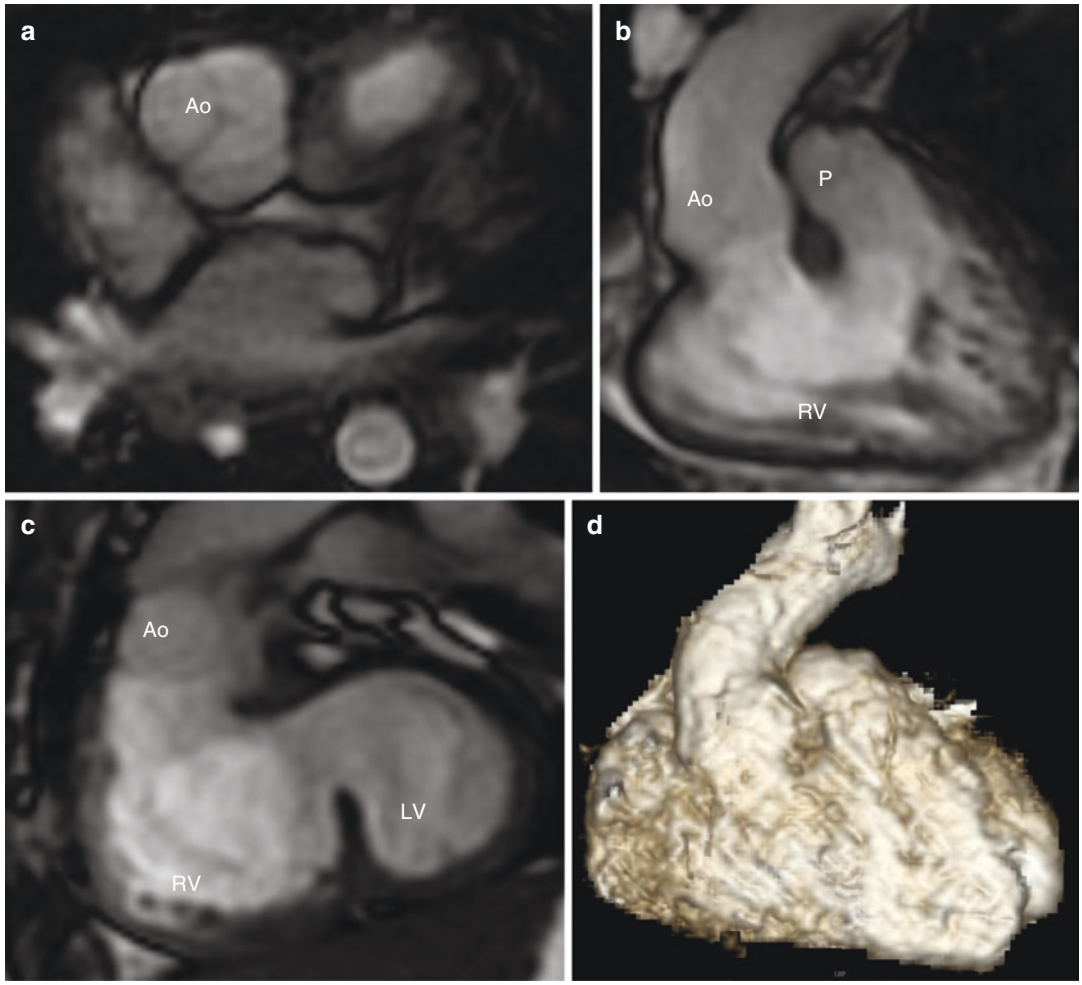

Fig. 15.33 An 8-year-old boy with DORV. Axial (**a**), outflow views (**b**, **c**) and MRA VRT (**d**) show DORV and large VSD—predominantly inlet in location, extending into subaortic/conoventricular region with most of the LV–Aorta route occupied by tricuspid valve tissue (**c**). Severely hypertrophied conal septum (**a**, **c**). Side-by-side great arteries (rightward Aorta, leftward PA) (**a**, **d**). He underwent successful surgery by tunneling of VSD to the aorta using e-PTFE patch, transatrial resection of the conal septum, and tricuspid valve repair. *Ao* aorta; *LV* left ventricle; *P* pulmonary artery; *RV* right ventricle (Ref to Videos 15.37, 15.38, 15.39, 15.40, 15.41, 15.42, 15.43, and 15.44)

stenosis, homograft obstruction, and coronary artery abnormalities after arterial switch (Figs. 15.36, 15.37, and 15.38). Injury to bundle of His which may run along the margin of VSD can lead to conduction abnormality including complete heart block.

15.12 Double Outlet Left Ventricle (DOLV)

In contrast to the double outlet right ventricle, DOLV is a rarity. Both great arteries arise from the left ventricle with bilaterally deficient

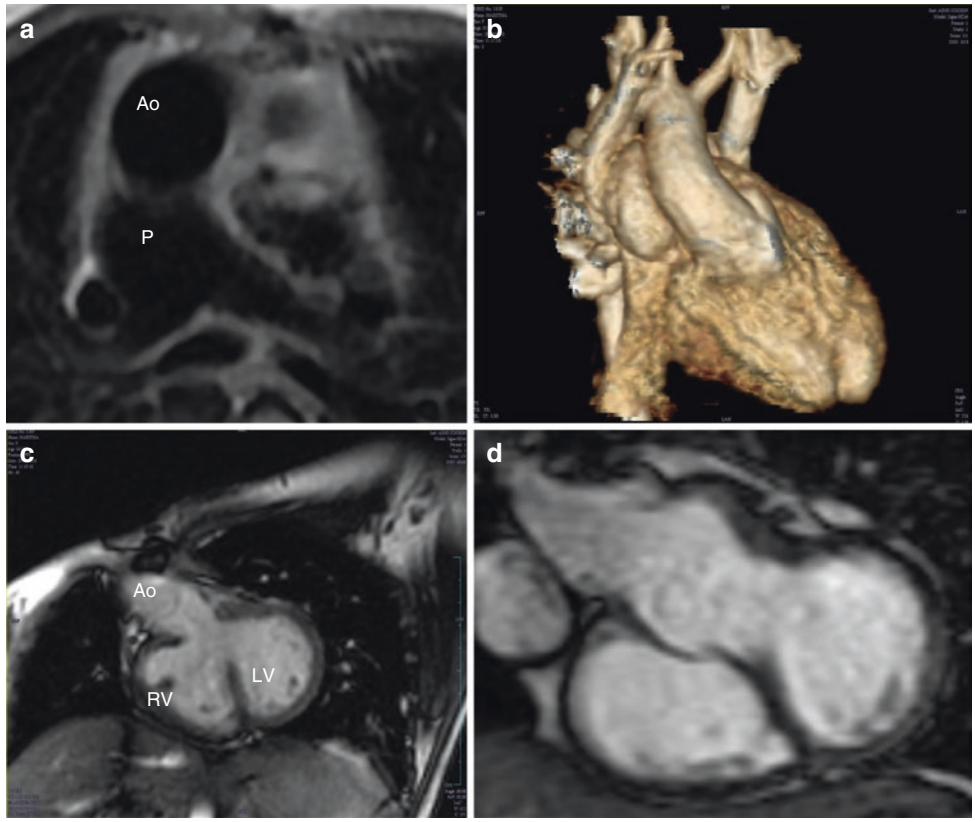

Fig. 15.34 A 12-year-old girl with DORV (Taussig–Bing anomaly), single large conoventricular subpulmonic VSD with mild inlet extension, dilated L-malposed aorta (**a**, **b**). There is a clear path between the LV and the aorta (routable VSD). Prominent subaortic conus and part of the Tricuspid Valve comes in path, but probably not enough to preclude VSD routing (**c**). She underwent routing of the VSD to the aorta using two GoreTex patches, infundibular resection, MPA division, and RV-PA conduit. Postoperative MRI (**d**) shows widely patent LV to aorta tunnel. *Ao* aorta; *LV* left ventricle; *P* pulmonary artery; *RV* right ventricle (Ref to Videos 15.45, 15.46, 15.47, 15.48, 15.49, 15.50, 15.51, 15.52, 15.53, and 15.54)

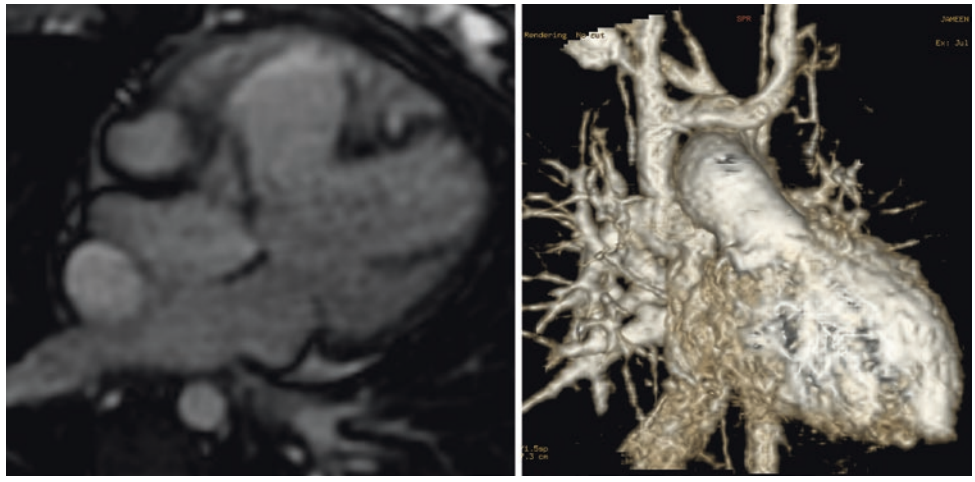

Fig. 15.35 A case of DORV underwent Fontan surgery because of inadequate RV size for biventricular repair (Ref to Videos 15.55, 15.56, 15.57, and 15.58)

Table 15.2 Management strategies based on variant of DORV

Type	Management
VSD type	VSD closure with LV to aorta routing within the first 6 months
TOF type	VSD closure with LV to aorta routing and relief of pulmonary obstruction in the age of 4 to 12 months
TGA type	Early corrective surgery with arterial switch, VSD closure – Alternatively Rastelli procedure—baffling of the LV to aortic valve and placement of a conduit from RV to pulmonary trunk
Single ventricle type	Fontan surgery

infundibulums. A high frequency of obstruction in the pulmonary outflow tract is found when the VSD is subaortic (Fig. 15.39). DOLV occurs most commonly in the form of atrial situs solitus with atrioventricular (AV) concordance but is often associated with cardiac anomalies such as a VSD, an atrial septal defect, pulmonary stenosis, right ventricular hypoplasia, patent ductus arteriosus, and tricuspid atresia [35, 36].

15.13 Conclusion

DORV is an extremely heterogeneous group of malformations that require a comprehensive diagnostic approach for tailored surgical man-

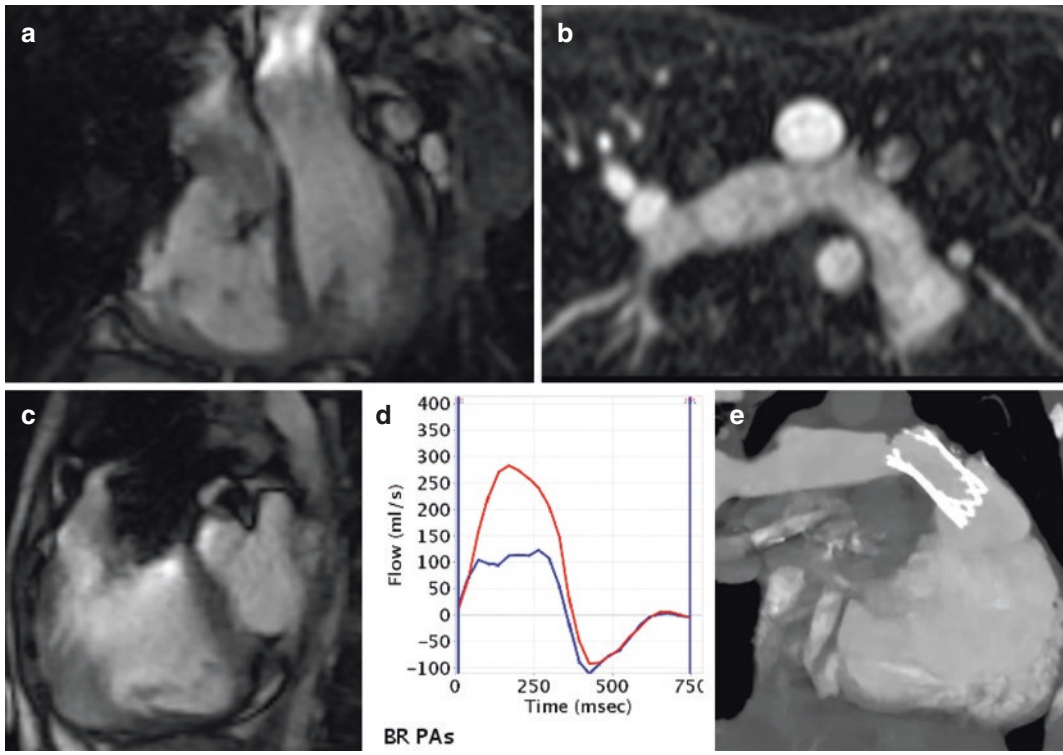

Fig. 15.36 Follow-up case of DORV underwent multiple staged procedures leading to intracardiac repair, RV to PA conduit, and RVOT stenting. CMR show a patent VSD patch without any residual VSD (outflow view-**a**), confluent unobstructed branch pulmonary arteries (MRA-**b**), significant pulmonary regurgitation (PC flow curve-**d**) (calculates as about 40%). RV to PA conduit stent cause severe artifact on MRI (**c**) and better evaluated by CT (**e**)

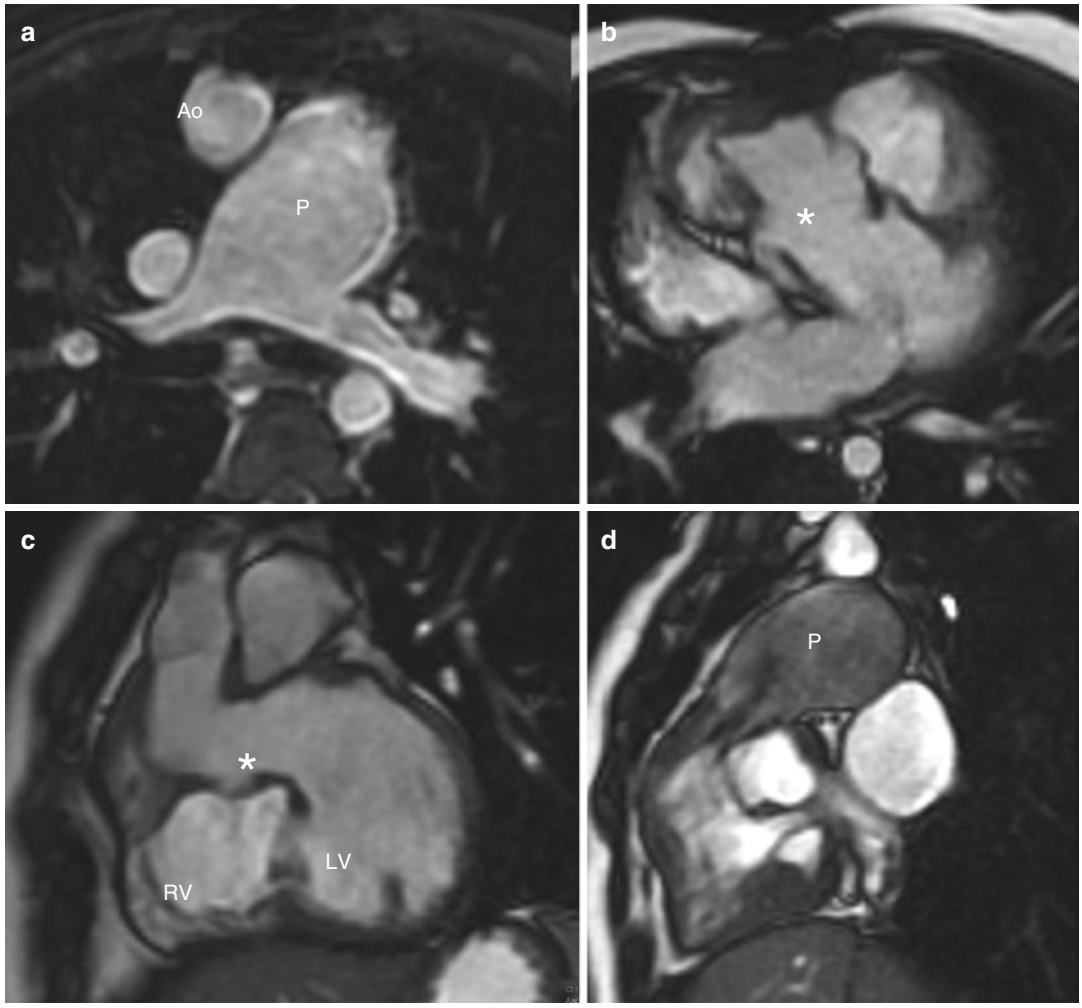

Fig. 15.37 A patient with DORV, large inlet VSD, moderate size CV-VSD underwent multiple e-PTFE patches. Postoperative MRI shows confluent branch pulmonary arteries (**a**), widely patent LV to aorta tunnel (* in **b**, **c**), subpulmonic obstruction (**d**) and dilated MPA. *Ao* aorta; *LV* left ventricle; *P* pulmonary artery; *RV* right ventricle

agement. DORV with subaortic VSD and pulmonary stenosis resembles that of TOF. Taussig–Bing type of DORV is treated similarly to TGA. The location of VSD, as seen from the side of the right ventricle, needs to be described. Other essential anatomic information analyzed include: atrial arrangements, atrioventricular connection, AV valve morphology including the attachment of subvalvular apparatus, ventriculoarterial connection, morphology of outflow tract obstruction, the relationship of great arteries, and other associated anomalies.

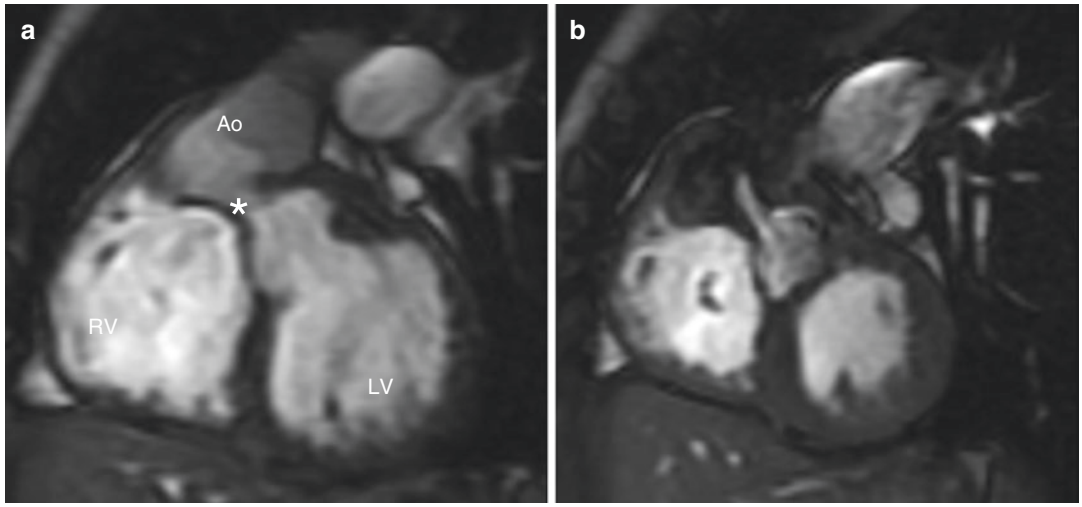

Fig. 15.38 A 10-year-old child status post DORV repair (Complex Kawashima intraventricular tunneling with fenestrated VSD closure). Short-axis cine images during diastole (**a**) and systole (**b**) show subvalvular aortic stenosis (*) in the LV–Aorta tunnel resulting from the indentation of the VSD patch and the presence of subaortic conal tissue. *Ao* aorta; *LV* left ventricle; *RV* right ventricle (Ref to Videos 15.59, 15.60, 15.61, 15.62, 15.53, and 15.64)

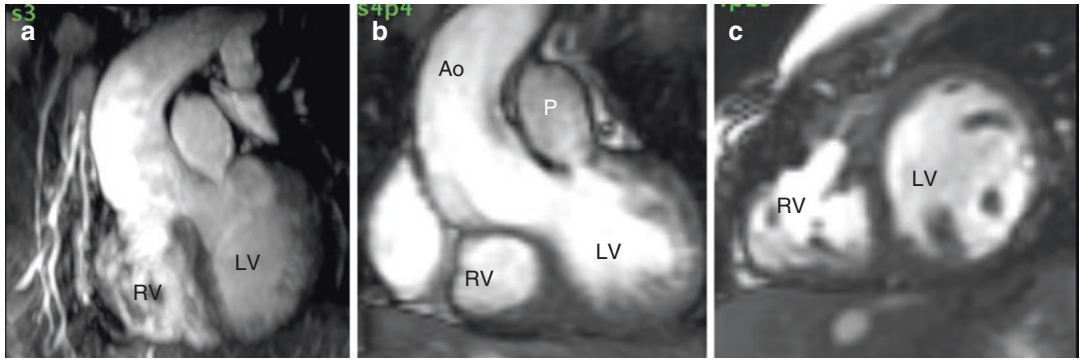

Fig. 15.39 A 5-year-old boy, outflow views (**a**, **b**) and short axis MRI (**c**) showing DOLV (PA from LV, Aorta overriding the ventricles), large conoventricular VSD (**a**) with inlet extension, severe pulmonary stenosis (**a**, **b**), relatively small RV (**c**). Since the post-tunneling estimated RV volume was low, he underwent Fontan surgery. *Ao* aorta; *LV* left ventricle; *P* pulmonary artery; *RV* right ventricle

References

1. Walters HL III, Mavroudis C, Tchervenkov CI, Jacobs JP, Lacour-Gayet F, Jacobs ML. Congenital heart surgery nomenclature and database project: double outlet right ventricle. Ann Thorac Surg. 2000;69:S249–63.
2. Lev M, Bharati S, Meng L, Liberthson RR, Paul MH, Idriss F. A concept of double outlet right ventricle. J Thorac Cardiovasc Surg. 1972;64:271–81.
3. Wilcox BR, Ho SY, Macartney FJ, Becker AE, Gerlis LM, Anderson RH. Surgical anatomy of double outlet right ventricle with situs solitus and atrioventricular concordance. J Thorac Cardiovasc Surg. 1981;92:405–17.
4. Abernethy J. Surgical and physiological essays. Part II. London: James Evans, Pater-Noster-Row; 1793. p. 157–65.
5. Taussig HB, Bing RJ. Complete transposition of the aorta and a levoposition of the pulmonary artery. Am Heart J. 1949;37:551–9.
6. Witham AC. Double outlet right ventricle. A partial transposition complex. Am Heart J. 1957;53:928–39.

7. Chen SJ, Lin MT, Liu KL, Chang CI, Chen HY, et al. Usefulness of 3D reconstructed computed tomography imaging for double outlet right ventricle. J Formos Med Assoc. 2008;107(5):371–80.
8. Shi K, Yang Z, Chen J, Zhang G, Xu H, et al. Assessment of double outlet right ventricle associated with multiple malformations in pediatric patients using retrospective ECG-gated dual-source computed tomography. PLoS One. 2015;10(6):e0130987.
9. Yoo SJ, Spray T, Austin EH 3rd, Yun TJ, van Arsdell GS. Hands-on surgical training of congenital heart surgery using 3-dimensional print models. J Thorac Cardiovasc Surg. 2017;153:1530–40. https://doi.org/10.1016/j.jtcvs.2016.12.054.
10. Guo W, Lin ML, Gu ZQ, et al. Double outlet right ventricle, a clinical-roentgenologic-pathologic study of 28 consecutive patients. Chest. 1984;85:526–32.
11. Van Praagh R, Geva T, Kreutzer J. Ventricular septal defects: how shall we describe, name, and classify them? J Am Coll Cardiol. 1989;14:1298–9.
12. Sebastian L, Erwin O, Lars H, et al. Pre- and postoperative evaluation of congenital heart disease in children and adults with 64-section CT. Radiographics. 2007;27:829–46.
13. Aoki M, Forbess JM, Jonas RA, Mayer RE, Castaneda AR. Results of biventricular repair for double outlet right ventricle. Thorac Cardiovasc Surg. 1984;107:338–50.
14. Kleinert S, Sano T, Weintraoub RG, Karl TR, Wilkinson JL. Anatomic features and surgical strategies in double outlet right ventricle. Circulaion. 1997;96:1233–9.
15. Belli E, Serraf A, Lacour Gayet F, Inamo J, Houyet L, Bruniaux J, Planché C. Surgical treatment of subaortic stenosis after biventricular repair of double outlet right ventricle. J Thorac Cardiovasc Surg. 1996;122:1570–80.
16. Brown JW, Ruzmetov M, Okada Y, Vijay P, Turrentine MW. Surgical results in patients with double outlet right ventricle: a 20 year experience. Ann Thorac Surg. 2001;72:630–5.
17. Bradley T, Karamlou T, Kulik A, Mitrovic B, Vigneswara T, Jaffer S, Glasgow PD, Williams WG, VanArsdell G, McCrindle BW. Determinants of repair type, reintervention, and mortality in 393 children with double outlet right ventricle. J Thorac Cardiovasc Surg. 2007;134:969–73.
18. Lincoln C, Anderson RH, Shinebourne EA, English TAH, Wilkinson JL. Double outlet right ventricle with l-malposition of the aorta. Br Heart J. 1975;37:453–63.
19. Belli E, Serraf A, Lacour-Gayet F, Hubler M, Zoghby J, Houyel L, Planche C. Double outlet right ventricle with non-committed ventricular septal defect. Eur J Cardiothorac Surg. 1999;15:747–52.
20. Edwards JE, James JW, Dushane JW. Congenital malformation of the heart; origin of transposed great vessels from the right ventricle associated with atresia of the left ventricular outlet, double orifice of the mitral valve and single coronary artery. Lab Investig. 1952;1:197–207.
21. Lavoie R, Sestier F, Gilbert G, Chameides L, Van Praagh R, Grondin P. Double outlet right ventricle with left ventricular outflow tract obstruction due to small ventricular septal defect. Am Heart J. 1971;82:290–9.
22. Mazzucco A, Faggian G, Stellin G, Bortolotti U, Livi U, Rizzoli G, Gallucci V. Surgical management of double-outlet right ventricle. J Thorac Cardiovasc Surg. 1985;90:29–34.
23. Belli E, Serraf A, Lacour-Gayet F, et al. Double-outlet right ventricle with non-committed ventricular septal defect. Eur J Cardiothorac Surg. 1999;15:747–52.
24. Tabry IF, Mcgoon DC, Danielson GK, et al. Surgical management of double outlet right ventricle associated with atrioventricular discordance. J Thorac Cardiovasc Surg. 1978;76:336–44.
25. Anjos RT, Ho SY, Anderson RH. Surgical implications of juxtaposition of the atrial appendages. A review of forty-nine autopsied hearts. J Thorac Cardiovasc Surg. 1990;99:897–904.
26. Lacour-Gayet F. Biventricular repair of double outlet right ventricle with noncommitted ventricular septal defect. Semin Thorac Cardiovasc Surg Pediatr Card Surg Annu. 2002;5:163–72.
27. Farooqi KM, Uppu SC, Nguyen K. Application of virtual three-dimensional models for simultaneous visualization of intracardiac anatomic relationships in double outlet right ventricle. Pediatr Cardiol. 2016;37(1):90–8.
28. Yim D, Dragulescu A, Ide H, et al. Essential modifiers of double outlet right ventricle - revisit with endocardial surface images and 3-dimensional print models. Circ Cardiovasc Imaging. 2018;11:e006891.
29. Harvey JC, Sondheimer HM, William WG, et al. Repair of double outlet right ventricle. J Thoracic Cardiovasc Surg. 1977;73:611–5.
30. Brown JW, Ruzmetov M, Okada Y, Vijay P, Turrentine MW. Surgical results in patients with double outlet right ventricle: a 20-year experience. AnnThorac Surg. 2001;72(5):1630–5.
31. Wetter J, Sinzobahamvya N, Blaschczok HC, et al. Results of arterial switch operation for primary total correction of the Taussig-Bing anomaly. Ann Thorac Surg. 2004;77(1):41–6. discussion 47
32. Belli E, Serraf A, Lacour-Gayet F, et al. Surgical treatment of subaortic stenosis after biventricular repair of double-outlet right ventricle. J Thorac Cardiovasc Surg. 1996;112(6):1570–8.
33. Lacour-Gayet F, Haun C, Ntalakoura K, Belli E, Houyel L, Marcsek P, et al. Biventricular repair of

double outlet right ventricle with non-committed ventricular septal defect (VSD) by VSD rerouting to the pulmonary artery and arterial switch. Eur J Cardiothorac Surg. 2002;21:1042–8.
34. Delius RE, Rademecker MA, de Level MR, et al. Is a high risk biventricular repair always preferable to conversion to a single ventricle repair? J Thorac Cardiovasc Surg. 1996;112:1561–9.
35. Bharati S, Lev M, Stewart R, McAllister H, Kirklin J. The morphologic spectrum of double outlet left ventricle and its surgical significance. Circulation. 1978;58:558–65.
36. Galal O, Hatle L, Al HZ. Changes of management in a patient with double outlet left ventricle. Cardiol Young. 1999;9:602–5.